INFORMATION TO USERS

This manuscript has been reproduced from the microfilm master. UMI films the text directly from the original or copy submitted. Thus, some thesis and dissertation copies are in typewriter face, while others may be from any type of computer printer.

The quality of this reproduction is dependent upon the quality of the copy submitted. Broken or indistinct print, colored or poor quality illustrations and photographs, print bleedthrough, substandard margins, and improper alignment can adversely affect reproduction.

In the unlikely event that the author did not send UMI a complete manuscript and there are missing pages, these will be noted. Also, if unauthorized copyright material had to be removed, a note will indicate the deletion.

Oversize materials (e.g., maps, drawings, charts) are reproduced by sectioning the original, beginning at the upper left-hand corner and continuing from left to right in equal sections with small overlaps.

Photographs included in the original manuscript have been reproduced xerographically in this copy. Higher quality 6" x 9" black and white photographic prints are available for any photographs or illustrations appearing in this copy for an additional charge. Contact UMI directly to order.

Bell & Howell Information and Learning
300 North Zeeb Road, Ann Arbor, MI 48106-1346 USA
800-521-0600

Fatty Acid Oxidation in Mitochondria: The Impact of Enzyme Organization and Aspects of Unsaturated Fatty Acids Degradation

by

Xiquan Liang

A dissertation submitted to the Graduate Faculty in Biochemistry in partial fulfillment of the requirements for the degree of Doctor of Philosophy

The City University of New York

2000

This manuscript has been read and accepted for the Graduate Faculty in Biochemistry in satisfaction of the dissertation requirement for the degree of Doctor of Philosophy.

March 22, 1999
Date

Chair of Examining Committee

March 22, 1999
Date

Executive Officer

Supervisory Committee

The City University of New York

ABSTRACTS

Fatty Acid Oxidation in Mitochondria: The Impact of Enzyme Organization and Aspects of Unsaturated Fatty Acids Degradation

by

Xiquan Liang

Adviser: Professor Horst Schulz

4-Bromotiglic acid, a novel inhibitor of β-oxidation, was developed as a tool for probing the cooperation between the membrane-bound and soluble β-oxidation systems of rat liver mitochondria. Long-chain fatty acids seem to be acted upon first by the membrane-bound β-oxidation system. The main transfer of intermediates between the two systems probably occurs after the length of the acyl chain has been shortened to 14 or 12 carbon atoms.

Differences between the oxidation of *cis* and *trans* fatty acids were observed in rat mitochondria. 5-*trans*-Tetradecenoyl-CoA was found to accumulate in the matrix of both rat heart and rat liver mitochondria during the oxidation of elaidoyl-CoA at a three-fold higher level than was 5-*cis*-tetradecenoyl-CoA which is derived from oleoyl-CoA. Other metabolites that accumulated were hexanoyl-CoA and dodecanoyl-CoA regardless of whether saturated or unsaturated long-chain acyl-CoAs served as substrates. The accumulation of these metabolites is possibly due to the organization of β-oxidation enzymes in the mitochondrial matrix.

The mitochondrial metabolism of conjugated fatty acids was investigated. 5,7-Dienoyl-CoAs are the expected metabolites of polyunsaturated fatty acids with

conjugated double bonds at odd-numbered position. After introduction of a 2-*trans* double bond, the resultant 2,5,7-trienoyl-CoA can either continue its pass through the β-oxidation cycle or be converted by Δ^3,Δ^2-enoyl-CoA isomerase to 3,5,7-trienoyl-CoA. The latter compound is isomerized by a novel enzyme, named $\Delta^{3,5,7},\Delta^{2,4,6}$-trienoyl-CoA isomerase, to 2,4,6-trienoyl-CoA that is a substrate of 2,4-dienoyl-CoA reductase and hence can be completely degraded via β-oxidation.

2,4-Dienoyl-CoA reductase from *E. coli* was found to be a novel Fe-S flavoprotein that contains 1 mole of FAD, 1 mole of FMN, 4 moles of Fe and 4 moles of labile sulfur per mole of enzyme. The reductase can be reduced by dithionite or NADPH, and also can undergo photoreduction. It needs approximately 5 electrons for its complete reduction, and requires the removal of 4 to 5 electrons for the oxidation of the reduced enzyme.

ACKNOWLEDGEMENTS

I would like to express my gratitude to my mentor, Dr. Horst Schulz, for his guidance and support. I also greatly appreciate the advice and the encouragement from my thesis committee. Special thanks are given to Dr. Colin Thorpe, professor at the University of Delaware, and Dr. Howard Sprecher, professor at Ohio State University, for their collaborations. I would like to thank my colleagues, especially Mr. Chin-hung Chu, for their assistance.

Finally I would like to thank my mother and my wife, Minling Liu, for their full support.

LIST OF TABLES

LIST OF FIGURES

TABLE OF CONTENTS

ABBREVIATIONS

ADP	Adenosine 5'-diphosphate
BSA	Bovine serum albumin
CoA	Coenzyme A
DEAE	Diethylamino ethyl
EDTA	Ethylenediaminetetraacetate
EGTA	Ethylene glycol bis-(aminoethyl ether) N', N-tetraacetic acid
FAD	Flavin adenine dinucleotide (oxidized)
FMN	Flavin mononucleotide (oxidized)
GC-MS	Gas chromatography and mass spectrometry
KPi	Potassium phosphate
NAD^+	Nicotinamide adenine dinucleotide (oxidized)
NADH	Nicotinamide adenine dinucleotide (reduced)
NADPH	Nicotinamide adenine dinucleotide phosphate (reduced)
PAGE	Polyacylamide gel electrophoresis
PMSF	Phenyl methane sulfonyl fluoride
SDS	Sodium dodecyl sulfate
TCA	Trichloroacetic acid
Tris-HCl	Tris(hydroxymethyl)aminomethane hydrochloride

INTRODUCTION

Fatty acid degradation in mitochondria requires the participation of two enzyme systems, each of which catalyzes a full cycle of β-oxidation (1). One set of enzymes with a preference for long-chain fatty acids is bound to the inner mitochondrial membrane and consists of very-long-chain acyl-CoA dehydrogenase and a trifunctional β-oxidation complex which harbors medium-chain and long-chain activities of enoyl-CoA hydratase, L-3-hydroxyacyl-CoA dehydrogenase, and 3-ketoacyl-CoA thiolase (Fig. 1). The second set consists of soluble matrix enzymes that are most active toward short-chain and medium-chain fatty acids, and are suspected to be in physical contact with the inner mitochondrial membrane (Fig. 1). Very-long-chain acyl-CoA dehydrogenase has been purified from rat liver, has native and subunit molecular weights of 150,000 and 71,000 respectively, and contains two moles of FAD per mole of enzyme (2). The very-long-chain acyl-CoA dehydrogenase acts preferably on longer chain length fatty acyl-CoAs including fatty acyl-CoAs with 22 and 24 carbon atoms (2). The short-chain acyl-CoA dehydrogenase is generally most active with butyryl-CoA (3,4). The medium-chain acyl-CoA dehydrogenase has a broad-chain length specificity that extends from butyryl-CoA or hexanoyl-CoA to myristoyl-CoA or palmitoyl-CoA (3,4). The spectrum of long-chain acyl-CoA dehydrogenase activities extends from hexanoyl-CoA or octanoyl-CoA to arachidonoyl-CoA with a maximum activity at or near lauroyl-CoA (3,4). It is speculated that matrix long-chain, medium-chain, and short-chain acyl-CoA dehydrogenases interact functionally with the soluble enoyl-CoA hydratase, L-3-hydroxyacyl-CoA dehydrogenase, and 3-ketoacyl-CoA thiolase present in the matrix. Based on the

hypothesis in Fig. 1, long-chain acylcarnitines that enter the matrix are acted upon by carnitine palmitoyltransferase II at the inner mitochondrial membrane to yield long-chain acyl-CoAs which first undergo one or more cycles of chain shortening catalyzed by the membrane-bound long-chain-specific β-oxidation system. Intermediate channeling on the trifunctional beta-oxidation complex from pig heart mitochondria has been reported (5). The resultant medium-chain intermediates are substrates of the matrix β-oxidation system. Intermediates that shift from one to the other β-oxidation system are expected to accumulate to a greater extent than other intermediates. Although investigations of inherited fatty acid oxidation disorders in humans have led to the conclusion that both enzyme systems are required for the β-oxidation of fatty acids (6), the cooperation of the two systems in the degradation of long-chain fatty acids remains largely unexplored.

The β-oxidation of typical polyunsaturated fatty acids requires the involvement of three auxiliary enzymes in addition to the enzymes that catalyze the four basic reactions of the β-oxidation spiral (Fig. 2). The auxiliary enzymes are Δ^3,Δ^2-enoyl-CoA isomerase (EC 5. 3. 3. 8), 2,4-dienoyl-CoA reductase (EC 1. 3. 1. 34), and $\Delta^{3,5}$,$\Delta^{2,4}$-dienoyl-CoA isomerase (dienoyl-CoA isomerase). Δ^3,Δ^2-Enoyl-CoA isomerase has been purified from rat liver (7,8), rat heart (8), and bovine liver (9). This enzyme is a homodimer with a subunit molecular weight of close to 30,000 (7,8,9) and catalyzes the isomerization of 3-*trans*- and 3-*cis*-enoyl-CoAs to 2-*trans*-enoyl-CoAs. 2,4-Dienoyl-CoA reductase from bovine liver is a homotetramer with a molecular weight of 124,000 (10), whereas 2,4-Dienoyl-CoA reductase from *E. coli* is a monomer with a molecular weight of around 72,000 (10). $\Delta^{3,5}$,$\Delta^{2,4}$-Dienoyl-CoA isomerase was purified from rat liver and found to have a subunit molecular weight of 32,000 (11). These auxiliary enzymes catalyze either

the reduction or isomerization of double bonds that are in close proximity to the thioester function as a result of acyl chain shortening. Consequently, double bonds either are reductively removed or are shifted to yield 2-*trans*-enoyl-CoAs which are intermediates of the β-oxidation spiral. Polyunsaturated fatty acid with conjugated double bonds may yield intermediates with more extended chromophores. For example, a fatty acid with two conjugated double bonds at even-numbered positions is assumed to be chain shortened by β-oxidation to 4,6-dienoyl-CoA and then converted to 2,4,6-trienoyl-CoA by acyl-CoA dehydrogenase. The further metabolism of this intermediate is facilitated by 2,4-dienoyl-CoA reductase that catalyzes the reduction of one double bond of the 2,4-diene portion of the 2,4,6-trienoyl-CoA chromophore (12). The β-oxidation of a fatty acid with two conjugated double bonds at odd-numbered positions would produce a 5,7-dienoyl-CoA, which may be dehydrogenated by acyl-CoA dehydrogenase to 2,5,7-trienoyl-CoA. The latter compound may be chain shortened to 3,5-dienoyl-CoA or isomerized to 3,5,7-trienoyl-CoA by Δ^3,Δ^2-enoyl-CoA isomerase. The further metabolism of 3,5,7-trienoyl-CoA would require the action of a $\Delta^{3,5,7},\Delta^{2,4,6}$-trienoyl-CoA isomerase, an enzyme that so far has not been described.

2,4-Dienoyl-CoA reductase is the key enzyme in the degradation of unsaturated fatty acids with even-numbered double bonds. This enzyme catalyzes the NADPH-dependent reduction of 2,4-dienoyl-CoA esters. In mammals, 2,4-dienoyl-CoA is reduced to 3-*trans*-enoyl-CoA (13) that in turn is isomerized to 2-*trans*-enoyl-CoA by Δ^3,Δ^2-enoyl-CoA isomerase. In contrast, in *E. coli* 2-*trans*-enoyl-CoA is the product of the reduction of 2,4-dienoyl-CoA. Bovine liver 2,4-dienoyl-CoA reductase was found to be a homotetramer, whereas *E. coli* 2,4-dienoyl-CoA reductase is a monomer with FAD

as a cofactor (13). Recently, *E. coli* 2,4-dienoyl-CoA reductase was cloned and overexpressed (14). A comparison of the *E. coli* and rat 2,4-dienoyl-CoA reductases did not reveal significant sequence similarities.

The reduction of 2,4-dienoyl-CoA by the mammalian reductase involves a 2,5 hydrogen addition to yield 3-enoyl-CoA, whereas the *E. coli* reductase probably catalyzes a 4,5 addition thereby producing 2-enoyl-CoA. These conclusions are supported by the following observations. Mizugaki et al. (15,16) reported that one deuterium atom was incorporated at carbon 5 of the 3-decenoate product when 4S-[4-^{2}H] NADPH served as the coenzyme of the bovine liver reductase. However, two deuterium atoms were incorporated at carbon 4 and carbon 5 of 2-decenoate when 2,4-decadienoyl-CoA was reduced by *E. coli* 2,4-dienoyl-CoA reductase in the presence of NADPH and ^2H_2O. However, these results were ambiguous because the partial incorporation of a deuterium atom was observed at carbon 2 or carbon 3 of 2-decenoate (16).

Polyunsaturated fatty acids with conjugated double bonds, as for example conjugated linoleic acids and *trans* fatty acids, are formed during the partial catalytic hydrogenation of fats (17) and in ruminants (18). Consequently, they are constituents of the human diet and they are substrates of β-oxidation. A complete understanding of their degradation by β-oxidation is essential for analyzing problems caused by the consumption of large amounts of such fatty acids and by their presence in the diet of patients with impaired β-oxidation due to inherited disorders or myocardial ischemia.

One aim of this study was to design, synthesize, and characterize an inhibitor that would irreversibly inactivate the long-chain specific β-oxidation system in intact rat liver mitochondria. Such an inhibitor would then be used to investigate the cooperation

between the two mitochondrial β-oxidation systems. A complementary approach was based on analyzing intermediates that accumulate in the matrix of mitochondria during the β-oxidation of various acyl-CoA substrates.

The second aim was the elucidation of the pathway in rat liver for the β-oxidation of polyunsaturated fatty acids with conjugated double bonds at odd-numbered carbon atoms and the characterization of 2,4-dienoyl-CoA reductase from *E. coli*.

EXPERIMENTAL PROCEDURES

Materials - CoASH, NADH, NADPH, ADP, FAD, FMN, stearoyl-CoA, oleoyl-CoA, elaidoyl-CoA, palmitoyl-CoA, pentadecanoyl-CoA, decanoyl-CoA, butyryl-CoA, all acylcarnitines, nonanoic acid, defatted BSA, *S. aureus* (Cowan Strain), catalase, acyl-CoA oxidase from *Arthrobacter* species, Q-Sepharose, Polybuffer Exchanger 94, Polybuffer 96, Reactive Red 120, Sepharose CL-6B, DEAE-cellulose, silica gel (70- to 230-mesh), phenylmethylsulfonyl fluoride, polyethylene glycol with an average molecular weight of 8,000, iron atomic absorption standard solution, N, N-dimethyl-p-phenylenediamine, 3-(2-pyridyl)-5,6-bis(4-phenyl sulfonic acid)-1,2,4-triazine (Ferrozine), and all standard biochemicals were obtained from Sigma. 2',5'-ADP-Sepharose 4B was purchased from Pharmacia Biotechnology, Inc. 2-Methyldecanoic acid was bought from Narchem Corp. (Chicago, IL). TCI America (Portland, OR) was the source of 2-bromopropionic acid *tert*-butyl ester. 2-*trans*,4-*trans*-Decadienal and 4-*cis*-decenal were purchased from ICN Pharmaceuticals. (4-

Carboxybutyl)triphenylphosphonium bromide, *trans*-2-pentenal, lithium bis(trimethylsilyl)amide, and chloroacetaldehyde were obtained from Fisher. Boron trichloride-methanol was obtained from SUPELCO. Octyl aldehyde, *trans*-cinnamaldehyde, triphenylphosphine, and hexadecyltributylphosphonium bromide were purchased from Aldrich. hydroxyapatite, the dye reagent for protein assays, and materials for immunoblotting, including the goat anti-rabbit IgG conjugated with alkaline phosphatase, were bought from Bio-Rad Laboratories. The multifunctional enzyme I from rat liver peroxisomes (19,20), enoyl-CoA hydratase (crotonase) from bovine liver (21), enoyl-CoA isomerase from rat liver (8), dienoyl-CoA isomerase from rat liver (11), and L-3-hydroxyacyl-CoA dehydrogenase from pig heart (22) were purified as described. Rabbit antiserum to rat liver dienoyl-CoA isomerase was raised by Pocono Rabbit Farms and Laboratory, Canadensis, PA. Deazaflavin was a gift from Dr. Colin Thorpe. Methyl 5-*cis*-octenoate, generously provided by Dr. H. Sprecher, Ohio State University, was saponified as described (23) to yield 5-*cis*-octenoic acid. 2-*trans*,4-*trans*-Decadienoic acid and 4-*cis*-decenoic acid were prepared from 2-*trans*,4-*trans*-decadienal and 4-*cis*-decenal, respectively, by oxidation with Ag_2O as described in principle by Thomason et al. (24). 5-Phenyl-2,4-pentadienoic acid was obtained by reacting cinnamaldehyde with malonic acid using a general procedure described by Linstead et al. (25). 3-*trans*-Decenoic acid was prepared in a similar way except that triethanolamine was used as solvent instead of pyridine.

All CoA derivatives were synthesized by the mixed-anhydride method as described by Fong and Schulz (26). Concentrations of thioesters except for 3-ketooctanoyl-CoA were determined by the method of Ellman (27) after cleaving the

thioester bond with hydroxylamine at pH 7. 3-Ketooctanoyl-CoA was prepared from 2-octynoyl-CoA as described in principle by Thorpe (28). 4-*cis*-Decenoyl-CoA was enzymatically converted to 2-*trans*,4-*cis*-decadienoyl-CoA by acyl-CoA oxidase in the presence of catalase as described by Yang et al. (29). 2-*trans*,4-*cis*-Decadienoyl-CoA was further purified by HPLC (30). 3,5-Octadienoyl-CoA and 3,5,7-decatrienoyl-CoA were prepared by the combined actions of acyl-CoA oxidase and peroxisomal trifunctional enzyme as described by Luo et al. (11). 2,5,7-decatrienoyl-CoA was prepared by dehydrogenating 5,7-decadienoyl-CoA with acyl-CoA oxidase at pH 9 (31).

Methods

Synthesis of 4-Bromotiglic Acid

The synthesis of 4-bromotiglic acid (Fig. 3, compound 7) was based on a synthetic approach outlined by Stotter and Hill (32). One of the required building blocks was (carb-*tert*-butoxyethylidene)-triphenylphosphorane (Fig. 3, compound 3) which was prepared from triphenylphosphine (26 g) and *tert*-butyl 2-bromopropionate (Fig. 3, compound 1) (10.6 g) in a 7:3 mixture of benzene and toluene (33,34). After the reaction mixture was stirred for 3 days at room temperature, the solvent was removed under reduced pressure and the residue was ground up in anhydrous ether. The crude phosphonium salt was dissolved in cold water and converted to the corresponding phosphorane by titrating the solution with 1 N NaOH to beginning alkalinity as indicated by phenolphthalein while simultaneously extracting the formed phosphorane into ether. After removal of the ether, 8 g (40%) of (carb-*tert*-butoxyethylidene)triphenylphosphorane was obtained. The product was further purified

by recrystallization from hot ethyl acetate by the addition of petroleum ether. The final product was reacted with chloroacetaldehyde in a Wittig reaction to yield *tert*-butyl 4-chloro-2-methylbut-2-enoate (Fig. 3, compound 5) (32). The commercial preparation of aqueous chloroacetaldehyde (15 g) was dehydrated by mixing it with 60 ml of CH_2Cl_2 and keeping it over anhydrous $MgSO_4$ for 1 h. After removal of the drying agent by filtration, the filtrate was combined with (carb-*tert*-butoxyethylidene)triphenyl-phosphorane (6.5 g) and heated under reflux for 4 h. After evaporating the solvent, the residue was extracted three times with a 1:1 mixture of petroleum ether and ether. The pooled extracts were applied to a silica gel column which was equilibrated and developed with a 1:1 mixture of petroleum ether and ether. *tert*-Butyl-4-chloro-2-methyl-but-2-enoate, which was eluted first, was detected by thin-layer chromatography. Fractions containing this compound were combined and freed of solvent to yield 2.5 g (79% yield) of product. The mass spectrum of the product revealed the presence of two protonated molecular ions with *m/z* of 191 and 193 in a ratio of 3:1 corresponding to the isotopic mixture of the chlorinated ester. *tert*-Butyl 4-chloro-2-methylbut-2-enoate was converted to the bromo-substituted ester by reacting the former compound (2 g) with lithium bromide (18 g) dissolved in acetone for 12 h. After evaporating the acetone under reduced pressure, the residue was extracted three times with petroleum ether. The resultant *tert*-butyl 4-bromo-2-methylbut-2-enoate (Fig. 3, compound 6) was hydrolyzed under acidic, not alkaline, conditions to avoid the likely hydrolysis of the bromine residue. For this purpose, the ester (1.7 g) was added to a mixture of hexadecyltributylphosphonium bromide (0.367 g) and 10 M aqueous sulfuric acid (3.6 ml) and stirred for 4 h at 25 °C. The resultant white-gray precipitate was isolated by

filtration and washed with a small amount of petroleum ether. After recrystallization from petroleum ether/ether, 4-bromotiglic acid (Fig. 3, compound 7) (0.8 g; 62% yield) was obtained with a mp of 92.5-93.5 °C in good agreement with a mp of 93.4-94.8 °C reported by Löffler et al. (35). The proton NMR spectrum in $CDCl_3$ showed three signals: 1.93 (s, 3, H-Cβ'), δ 4.04 (d, 2, H-Cγ), and δ 7.05 (m, 1, H-Cβ). NOE measurements did not show an enhancement of the signal corresponding to the H-Cβ proton upon irradiation of the sample at the frequency of the H-Cβ' protons. This observation agrees with an E configuration of the double bond, which was predicted by the synthetic approach (32). The mass spectrum revealed the presence of two protonated molecular ions with *m/z* values of 179 and 181, in a 1:1 ratio, reflecting the isotopic mixture of 4-bromotiglic acid.

Synthesis of 5,7-Decadienoic Acid

5,7-Decadienoic acid was synthesized by a Wittig reaction using the procedure described by Maryanoff et al. (36). Twenty mmol of (4-carboxybutyl) triphenylphosphonium bromide in 10 ml of dry tetrahydrofuran was reacted under N_2 with 42 mmol of lithium bis(trimethylsilyl)amide in 42 ml of tetrahydrofuran at room temperature with stirring. After 15 min, 16 mmol of *trans*-2-pentenal in 10 ml of tetrahydrofuran was added slowly. The color of the reaction changed from red to yellow. After 60 min, 50 ml water were added to quench the reaction. Mixture was extracted with ether to remove the unreacted aldehyde. The aqueous solution was acidified with 10% HCl, and extracted with ether. The combined ether extracts were extracted with water, dried over anhydrous Na_2SO_4, and concentrated to 0.82 g of 5,7-decadienoic acid

(~30% yield). The structure of the product was confirmed by mass spectrometry which showed the expected ($M + NH_4^+$) peak at 186.

Isolation of Rat Mitochondria from Rat Liver or Rat Heart and Respiration Measurements

Rat liver mitochondria were isolated as described by Nedergaard and Cannon (37). Rat heart mitochondria were isolated by the procedure of Chappell and Hansford (38). Protein concentrations of the mitochondrial suspension were determined by the Bradford method (39) with bovine serum albumin as the protein standard. For respiration measurements with rat liver, 1.5 mg of rat liver mitochondria were incubated in 1.9 ml of a basal medium containing 20 mM Tris-HCl (pH 7.4), 4 mM potassium phosphate, 0.1 M KCl, 4 mM $MgCl_2$, 0.1 mM EGTA, BSA (0.5 mg/ml), and 0.5 mM L-malate. In the case of rat heart mitochondria, 1 mg of heart mitochondria was incubated in 1.9 ml of a basal medium containing 33 mM Tris-HCl (pH 7.4), 2 mM potassium phosphate, 0.11 M KCl, 2 mM $MgCl_2$, 0.1 mM EGTA, BSA (0.5 mg/ml), and 0.5 mM L-malate. L-Carnitine (0.5 mM) was added to the incubation mixture when 15 μM of CoA derivatives were used as respiratory substrates with both rat liver and heart mitochondria. After preincubation for 2 min, respiration was initiated by the addition of 1 mM ADP and the indicated substrates. Rates of respiration were measured polarographically with a Clark oxygen electrode attached to a YS-oxygraph.

When the β-oxidation was inhibited, mitochondria were preincubated with 4-bromotiglic acid and ADP for 2 min before the respiration was stimulated with the respiratory substrates. When the reversibility of the inhibition caused by 4-bromotiglic

acid was evaluated, mitochondria were incubated with the inhibitor and ADP for 2 min. The mitochondrial suspension was then centrifuged at 13000 g for 30 s and the pellet was resuspended in the incubation medium except that the inhibitor was omitted. Respiration was initiated by the addition of substrate.

In order to determine the enzyme activities in mitochondria preincubated with or without 4-bromotiglic acid, rat liver mitochondria were incubated with various concentrations of 4-bromotiglic acid for 2 min under conditions used to measure respiration except that the substrate of fatty acid oxidation was omitted. Samples were quickly frozen in a dry ice/methanol bath and stored at –80 °C until assayed.

Studies of Metabolic Intermediates

When metabolic intermediates were studied, the above incubation mixture was scaled up to 20 ml. The reaction was terminated by the addition of 25 ml methanol at the indicated time. After addition of an internal standard, the suspension was centrifuged at 17,500 g for 15 min. The supernatant was diluted five-fold before it was passed slowly through a C_{18} Sep-Pak column. The bound CoA derivatives were eluted with 2.5 ml methanol. The extraction process was repeated, and 1 ml of 50 mM ammonium phosphate (pH 5.5) was added to the combined methanol. After removal of methanol under N_2 or reduced pressure, the remainder was applied to a Waters HPLC μBondapak C_{18} reverse-phase Column (30 cm x 3.9 mm) attached to a Waters gradient HPLC system. The absorbance of the effluent was monitored at 254 nm. Separation was achieved by linearly increasing the acetonitrile/H_2O (9:1, v/v) content of the 50 mM ammonium phosphate elution buffer (pH 5.5) from 20% to 80% in 30 min at a flow rate of 2 ml/min.

In some cases ammonium phosphate buffer was replaced by 10 mM potassium phosphate buffer (pH 5.5). Recovery of the metabolic intermediates was found to be around 35% with the internal standard as reference. To identify the metabolic intermediates, fractions were collected and freed of acetonitrile under reduced pressure. The resultant aqueous solution was mixed with an equal volume of 4 N KOH and kept at room temperature for 1 hr to hydrolyze the thioester bond. The mixture was adjusted pH to 1 with concentrated H_2SO_4 and extracted three times with ether. The combined extracts were dried over anhydrous $MgSO_4$ and filtered. After the ether was evaporated under N_2, the residue was treated with 1 ml of boron trichloride in methanol (12% w/w). 2, 2-Dimethoxypropane (100 ul) was added at this point. After the mixture was heated at 60 °C for 10 min, 1 ml of H_2O was added to terminate the reaction. The mixture was extracted three times with 1 ml of hexane each. The combined hexane extracts were dried over anhydrous $MgSO_4$ and filtered. The filtrate was concentrated under N_2 and then subjected to GC-MS analysis.

Identification of Metabolic Intermediates

In addition to being subjected to GC-MS analysis, suspected 5-*trans*-tetradecenoyl-CoA was treated with crotonase or a combination of acyl-CoA oxidase and crotonase. The products were analyzed by HPLC. 5-*trans*-Tetradecenoyl-CoA, which was chemically synthesized, was used as a standard.

Alternatively, fractions suspected of containing 5-*trans*-tetradecenoyl-CoA were freed of acetonitrile and further concentrated under reduced pressure. The dehydrogenation of metabolic intermediate was carried out by the addition of 0.1 U of

acyl-CoA oxidase. The isomerization of $\Delta^{2,5}$-tetradecadienoyl-CoA to $\Delta^{3,5}$-tetradecadienoyl-CoA, which was stimulated by the addition of 8 mU of $\Delta^{2,3}$-enoyl-CoA isomerase, was followed spectrophotometrically at 230 nm. The conversion of $\Delta^{3,5}$-tetradecadienoyl-CoA to $\Delta^{2,4}$-tetradecadienoyl-CoA, which was initiated by the addition of 4 mU of dienoyl-CoA isomerase, was followed by recording the increase in absorbance at 300 nm.

Determination of Enzyme Activities

Acyl-CoA dehydrogenase (EC 1.3.99.2 and EC 1.3.99.3), enoyl-CoA hydratases (EC 4.2.1.17 and EC 4.2.1.74), and L-3-hydroxyacyl-CoA dehydrogenase (EC 1.1.1.35) were assayed as described by Olowe and Schulz (40). The activities of acetoacetyl-CoA thiolase (EC 2.3.1.9) and 3-ketoacyl-CoA thiolase (EC 2.3.1.16) were determined as detailed by Binstock and Schulz (41).

Dienoyl-CoA isomerase was assayed spectrophotometrically by measuring the increase in absorbance at 300 nm on a Hitachi, model U-3010, spectrophotometer at 25 °C as described by Luo et al. (11). A typical assay mixture contained 20 μM 3,5-octadienoyl-CoA in 0.2 M KPi (pH 8.0). An extinction coefficient of 27,800 $M^{-1}cm^{-1}$ was used to calculate rates.

Trienoyl-CoA isomerase activity was determined by monitoring the absorbance increase at 337 nm. An extinction coefficient of 49,300 $M^{-1}cm^{-1}$ was used to calculate rates (12). A typical assay mixture contained 20 μM 3,5,7-decatrienoyl-CoA in 0.2 M KPi (pH 8.0) and enzyme to give an absorbance change of 0.04/min.

2,4-Dienoyl-CoA reductase was assayed spectrophotometrically by measuring

the oxidation of NADPH at 340 nm as described by Kunau (42). The assay mixture contained 50 mM potassium phosphate (pH 7.4), 0.1 mM NADPH, 25 μM 2-*trans*,4-*trans*-decadienoyl-CoA or 25 μM 5-phenyl-2,4-pentadienoyl-CoA, and purified 2,4-dienoyl-CoA reductase to give an absorbance change of 0.02 to 0.06 A/min. One unit of enzyme activity is defined as the amount of enzyme that catalyzes the conversion of 1 μmole of substrate to product per min.

Separation of Matrix and Membrane-Bound Thiolases

Rat liver mitochondria were incubated under conditions used for measuring respiration except that the respiratory substrate was omitted. Two samples were incubated for 3 min in the presence and absence of 30 μM 4-bromotiglic acid, respectively. The samples were immediately centrifuged at 7800 g for 10 min, and the pellets were suspended in 20 mM potassium phosphate (pH 7.0) containing 5 mM mercaptoethanol and 1 mM EDTA (buffer A), sonicated 8 times for 10 s each at 4 °C. The resultant suspensions were applied separately to DEAE-cellulose columns (1 x 10 cm) which had been equilibrated with buffer A. The columns were washed with buffer A containing 0.1 M KCl, and fractions of 2 ml were collected until protein ceased to be eluted. The columns were then developed with a 0.1-1 M KCl gradient in buffer A. Fractions of 1 ml were collected. Flow-through and gradient fractions were assayed for 3-hydroxyacyl-CoA dehydrogenase with 3-ketooctanoyl-CoA as substrate and for thiolase activities with acetoacetyl-CoA and 3-ketooctanoyl-CoA as substrates.

Purification of Trienoyl-CoA Isomerase from Pig Heart

Trienoyl-CoA isomerase was purified by the procedure developed for the purification of dienoyl-CoA isomerase (11). All operations were carried out at 4 °C. One frozen pig heart (330 g) was minced and blended with 1 liter of 20 mM KPi (pH 8.3) containing 5 mM mercaptoethanol, 1 mM EDTA, 1 mM EGTA, 1 mM benzamidine, and 0.5 mM PMSF (buffer A). The resulting suspension was centrifuged at 6500 x g for 20 min. Polyethylene glycol was added to the supernatant to achieve a final concentration of 10%. After keeping the suspension for 30 min, it was centrifuged at 6500 x g for 20 min. The pellet was resuspended in 200 ml of buffer containing 0.2 M KCl. After stirring overnight, the suspension was centrifuged at 100,000 x g for 1 h. The supernatant was diluted with four volumes of buffer A to lower the salt concentration and was applied to a Q-Sepharose column (2.5 x 50 cm) previously equilibrated with buffer A. The column was extensively washed with buffer A and then eluted with 600 ml of buffer A containing 0.2 M KCl. Fractions with trienoyl-CoA isomerase activity were combined and the pH was adjusted to 6.3 with 1 M KH_2PO_4. The mixture was applied to a hydroxyapatite column (2.5 x 25 cm) equilibrated with 5 mM KPi (pH 6.3) containing 5 mM mercaptoethanol, 1 mM EDTA, 1 mM EGTA, 1 mM benzamidine, and 0.5 mM PMSF (buffer B). The column was washed with buffer B containing 0.5 M KCl and then developed with a gradient made up of 300 ml of buffer B and 300 ml of buffer B containing 0.8 M KPi (pH 6.3). Fractions of 6 ml were collected and the active fractions were combined and concentrated in an Amicon concentrator with a YM-10 membrane. After dialyzing overnight against 25 mM ethanolamine-acetic acid (pH 9.4) containing 5 mM mercaptoethanol, 1 mM EDTA, 1 mM benzamidine, 0.5 mM PMSF and 20%

glycerol (buffer C), the sample was applied to a chromatofocusing column (1.5 x 25 cm) containing Polybuffer Exchanger 94 equilibrated with buffer C. The column was washed with buffer C and then developed with twelve columns of Polybuffer 96 adjusted to pH 6 with acetic acid. Fractions of 5 ml were collected, and the active fractions were combined and concentrated. After the sample was passed through a Sepharose CL-6B column (1.5 x 90 cm) equilibrated with 10 mM KPi (pH 7.0) containing 1 mM EDTA, 5 mM mercaptoethanol, and 25% glycerol (buffer D), the active fractions were combined and loaded on a Reactive Red 120 column (1.5 x 13 cm) previously equilibrated with buffer D. After washing with buffer D, the column was eluted with 15 μM 2-*trans*,4-*trans*-decadienoyl-CoA in buffer D. Fractions of 2 ml were collected and assayed for both dienoyl-coA and trienoyl-CoA isomerase activities. Active fractions were analyzed by SDS-PAGE and stained with Coomassie brilliant blue. The intensities of the bands were determined by gel scanning with a densitometer.

Metabolic Studies with 5,7-Decadienoyl-CoA

The formation of 3,5,7-decatrienoyl-CoA was monitored spectrophotometrically at 238 nm with a Hitachi, model U-3010, spectrophotometer. The incubation mixture contained 20 μM of 5,7-decadienoyl-CoA, acyl-CoA oxidase and peroxisomal trifunctional enzyme in 0.6 ml of 0.1 M potassium phosphate (pH 8). Scans were performed at different time interval. The isomerization of 3,5,7-decatrienoyl-CoA to 2,4,6-decatrienoyl-CoA was followed spectrophotometrically at 337 nm. HPLC-purified 3,5,7-decatrienoyl-CoA (20 μM) was incubated with soluble rat liver mitochondrial extract or partially purified dienoyl-CoA isomerase in 0.1 M KPi (pH 8).

The conversion was monitored at different times. The NADPH-dependent reduction of 2,4,6-decatrienoyl-CoA by partially purified rat liver 2,4-dienoyl-CoA reductase or purified *E. coli* 2,4-dienoyl-CoA reductase was followed spectrophotometrically at 340 nm. The incubation mixture contained 4 μM HPLC-purified 2,4,6-decatrienoyl-CoA, 0.1 mM NADPH, and 2,4-dienoyl-CoA reductase. The same amount of NADPH and enzyme were placed in the reference cuvette. Scans were performed at different time intervals.

The metabolism of 5,7-decadienoyl-CoA was also studied by HPLC. 5,7-Decadienoyl-CoA, which was purified by HPLC, was converted to 3,5,7-decatrienoyl-CoA by the combined actions of acyl-CoA oxidase and peroxisomal trifunctional enzyme I. The resultant 3,5,7-decatrienoyl-CoA was purified and isomerized to 2,4,6-decatrienoyl-CoA by partially purified dienoyl-CoA isomerase from rat liver. 2,4,6-Decatrienoyl-CoA was purified and reduced by purified *E. coli* 2,4-dienoyl-CoA reductase in the presence of NADPH. Samples were analyzed on a Waters μBondapak C_{18} reverse-phase column (30 cm x 3.9 mm) attached to a Waters gradient HPLC system. The absorbance of the effluent was monitored at 254 nm. Separation was achieved by linearly increasing the acetonitrile/H_2O (9:1, v/v) content of the 50 mM ammonium phosphate elution buffer (pH 5.5) from 20% to 55% in 30 min at a flow rate of 2 ml/min. For the purpose of purifying substrates, the desired fractions were collected. After evaporating the acetonitrile, the mixture was concentrated with Sep-Pak C_{18} cartridges.

Metabolism of 2,5,7-Decatrienoyl-CoA

The direct β-oxidation of 2,5,7-decatrienoyl-CoA was measured by incubating this compound at concentrations between 5 μM to 50 μM in 0.2 M KPi (pH 8.0) with 1 mM NAD^+, 0.3 mM CoASH and a soluble extract of rat liver mitochondria (4 μg/ml). The formation of NADH was determined fluorometrically by excitation at 340 nm and measuring the emission at 460 nm with a PTI spectrofluorimeter. The conversion of 2,5,7-decatrienoyl-CoA to 3,5,7-decatrienoyl-CoA was coupled to the isomerization of the latter compound to the 2,4,6-isomer in the presence of $\Delta^{3,5,7}$,$\Delta^{2,4,6}$-trienoyl-CoA isomerase (0.25 U/ml). 2,5,7-Decatrienoyl-CoA at concentrations between 5 μM to 60 μM in 0.2 M KPi (pH 8.0) was incubated with a soluble extract of rat liver mitochondria (4 μg/ml). The increase in the absorbance at 337 nm was measured spectrophotometrically. Rates were calculated based on an extinction coefficient of 49,300 $M^{-1}cm^{-1}$.

Immunoprecipitation

Dienoyl-CoA isomerase (2 μg) in 50 mM KPi (pH 7.0) containing 1 mM EDTA, 1 mM benzamidine and 5 mM mercaptoethanol was combined with various amounts of anti-dienoyl-CoA isomerase serum containing between 0 and 300 μg of protein. The total volume was 0.2 ml. The mixture was kept for 20 min at 25 °C and then combined with 0.2 ml of a suspension containing 10% (w/v) of *S. aureus* (Cowan strain). After the further incubation for 10 min at 25 °C, the mixture was centrifuged at 13,000 x g for 3 min. The supernatant was transferred to clean tubes and kept at 4 °C until being assayed for dienoyl-CoA isomerase and trienoyl-CoA isomerase activities.

Western Blotting

Aliquots of the fraction eluted from the Reactive Red 120 column were treated with SDS sample buffer, and then run on a 4-20% gradient gel for 60 min at 180 V. The gel, along with two pieces of filter paper and a nitrocellulose membrane, were soaked in transfer buffer (pH 9 to 9.4) containing 40 mM Tris-HCl, 39 mM glycerol, 37 ppm SDS and 20% (v/v) methanol for 30 min. Proteins were transferred to the nitrocellulose membrane for 25 min at 12 V by the semi liquid procedure. The membrane was soaked in blocking buffer containing 20 mM Tris-HCl (pH 7.4), 0.9% NaCl (TBS buffer) and 5% nonfat milk for 1 h. Thereafter it was washed with TBS buffer containing 0.2% nonfat milk for three times at 10 min intervals. Afterward, the membrane was incubated with 500-fold diluted rabbit antiserum against the rat liver dienoyl-CoA isomerase for 1 h, and then it was washed three times with TBS buffer containing 0.2% nonfat milk. The membrane was soaked in 2000-fold dilution of goat anti-rabbit IgG conjugated with alkaline phosphatase for 2 h. After the membrane was washed with TBS buffer containing 0.2% nonfat milk, it was incubated with developing buffer for 10 min at room temperature. The reaction was stopped by rinsing the membrane with deionized water and the membrane was dried in the air. The developing buffer contained 30 ml of Tris-saline (pH 9.5) stock solution, 0.2 ml of NBT stock solution and 0.1 ml of BCIP stock solution. Tris-saline stock solution contained 0.1 M Tris-HCl, 0.1 M NaCl, and 50 mM $MgCl_2$. NBT stock solution consisted of 5% of nitro blue tetrazolium chloride in 50% of N, N-dimethyl formamide. BCIP stock solution was made up of 5% of 5-bromo-4-chloro-3-indoyl phosphate p-toluidine in N, N-dimethyl formamide.

Expression and Purification of E. coli 2,4-Dienoyl-CoA Reductase

The fadH gene had been cloned into plasmid pNDH and expressed in *E. coli* BL21(DE3)plysS by He et al. (14). The *E. coli* BL21(DE3)plysS was grown in LB medium in the presence of ampicillin to an absorbance of about 1.0 at 600 nm, and then induced by 0.6 mM IPTG at 37°C under shaking at 200 rpm for 4 hours. Cells were harvested by centrifugation for 20 min at 5,000 rpm, and pellets were suspended in 20 mM potassium phosphate (pH 7.4) containing 1 mM EDTA, 10 mM 2-mercaptoethanol, 0.5 mM PMSF and 1 mM benzamidine. The suspension was sonicated 10 times for 20 sec each at 4 °C, and then centrifuged for 30 min at 15, 000 rpm. The purification of *E. coli* 2,4-dienoyl-CoA reductase was carried out as described by He et al. (14).

Study of cis-trans Isomerase Activity and Δ^3,Δ^2-Enoyl-CoA Isomerase

HPLC purified 2-*trans*,4-*cis*-decadienoyl-CoA was incubated with various amounts of purified *E. coli* 2,4-dienoyl-CoA reductase in 0.27 ml of 50 mM potassium phosphate buffer (pH 7.4). After 30 s of incubation, the reaction was terminated by the addition of 5 ul of concentrated HCl. Two minutes later, the pH of the mixture was readjusted to 5 with 4 N KOH and then centrifuged at 14,000 x g. The supernatant was analyzed by HPLC to detect the formation of 2-*trans*,4-*trans*-decadienoyl-CoA. Samples incubated in the absence of either *E. coli* 2,4-dienoyl-CoA reductase or 2-*trans*,4-*cis*-decadienoyl-CoA were used as controls. HPLC purified 2-*trans*,4-*trans*-decadienoyl-CoA was used as a reference.

The reduction of 2-*trans*,4-*trans*-decadienoyl-CoA was monitored spectrophotometrically. The incubation mixture contained 20 μM of 3-*trans*-decenoyl-CoA in the presence of either 0.1 mM NADPH or 0.1 mM $NADP^+$. The reaction was

terminated by acidification to pH 1-2. Two minutes later, the incubation mixtures was readjusted to pH 5.5, and then centrifuged. The supernatant was applied to HPLC. In order to distinguish 3-*trans*-decenoyl-CoA from 2-*trans*-decenoyl-CoA, crotonase was added to the formed products.

UV-VIS Spectrum of 5-Phenyl-2,4-pentadienoyl-CoA Bound to 2,4-Dienoyl-CoA Reductase

The spectrum of 20.8 μM *of E. coli* 2,4-dienoyl-CoA reductase in a 600 μl of 50 mM phosphate buffer (pH 7.4) was recorded before the addition of 1 ul of 0.45 mM 5-phenyl-2,4-pentadienoyl-CoA. The spectra of 5-phenyl-2,4-pentadienoyl-CoA and free 2,4-dienoyl-CoA reductase were taken separately. The spectrum of bound 5-phenyl-2,4-pentadienoyl-CoA was obtained by subtraction of the free *E. coli* reductase spectrum from the spectrum of the *E. coli* reductase 5-phenyl-2,4-pentadienoyl-CoA complex.

Determination of FAD, FMN, Iron and Labile Sulfide Contents in 2,4-Dienoyl-CoA Reductase from E. Coli

Commercial FMN and FAD were purified by HPLC and their concentrations were determined spectrophotometrically using extinction coefficients of 12.3 $mM^{-1}cm^{-1}$ for FMN, and 11.3 $mM^{-1}cm^{-1}$ for FAD. The *E. coli* reductase was denatured as described by Koziol (43). A solution of 0.48 nmol of *E. coli* reductase in 30 ul of 60 mM potassium phosphate (pH 7.4) was incubated with equal volume of 20% trichloroacetic acid at 0°C for 1 min, and then the mixture was centrifuged immediately at 14,000 x g for 1 min. The supernatant was neutralized with 4 M K_2HPO_4 before it was applied to an

HPLC column. In order to identify unknown cofactors, an enzyme solution, which had been treated with trichloroacetic acid (TCA) and neutralized with K_2HPO_4 as described above, was combined with an equimolar mixture of free FAD and FMN before it was applied to HPLC. In a control experiment, free FAD was treated with TCA in the same manner as the enzyme was treated.

Contents of FAD and FMN in *E. coli* reductase were determined by both HPLC and fluorescence spectrophotometer. The amount of FAD and FMN released from the reductase by 10% TCA was estimated from the area of the peaks with HPLC-purified FAD and FMN as standards. The contents of FAD and FMN in *E. coli* reductase were also determined fluorimetrically following the procedure described by Faeder and Siegel (44). *E. coli* reductase was diluted with standard buffer (0.1 M potassium phosphate, pH 7.7, containing 0.1 mM EDTA) and then immersed in a boiling water bath for 3 min. Fluorescence intensity was recorded using a Perkin-Elmer LS-5 Fluorescence Spectrophotometer with emission at 535 nm and excitation at 450 nm.

The amounts of iron and labile sulfur in *E. coli* reductase were determined according to the methods of Vanoni et al. (45) and Brumby et al. (46), respectively.

Effect of 8 M Guanidine Hydrochloride on E. coli Reductase

E. coli reductase (6.25 μM) was denatured in 0.1 M potassium phosphate buffer (pH 7.7) containing 0.1 mM EDTA and 8 M guanidine hydrochloride. An equimolar mixture of free FAD and FMN (6.25 μM each) in 8 M guanidine hydrochloride was used as a control. The purity of *E. coli* reductase was estimated by densitometry of all bands detected on a gel after SDS-PAGE. The concentration of reductase was calculated based

on the molecular weight of 72,550. An extinction coefficient of 34,400 $M^{-1}cm^{-1}$ for the native enzyme at 450 nm was calculated based on the measured absorbance and the established enzyme concentration.

Anaerobic Titration and Reduction of E. coli 2,4-Dienoyl-CoA Reductase

Concentrations of *E. coli* 2,4-dienoyl-CoA reductase were calculated by using an extinction coefficient of 34,400 $M^{-1}cm^{-1}$. Anaerobic experiments were performed in 1-ml capacity anaerobic cuvettes using the techniques summarized by Williams et al. (47). Visible and UV spectra were recorded with a Cary 219 spectrophotometer.

Several methods were tried to generate the flavosemiquinone state quantitatively from oxidized *E. coli* 2,4-dienoyl-CoA reductase. Photoreduction was carried out in 60 mM KPi (pH 7.4) containing 2 mM EDTA and 1 μM deazaflavin as described by Massey and Hemmerich (48). Back titration of the fully reduced enzyme with potassium ferricyanide was performed following the procedure described by Thorpe et al. (49). The concentration of ferricyanide was calibrated spectrophotometrically using an extinction coefficient of 1020 $M^{-1}cm^{-1}$ at 420 nm. The anaerobic titration of the enzyme with dithionite followed the procedure described by Mizzer and Thorpe (50). The concentration of dithionite was standardized with FAD, the concentration of which was determined spectrophotometrically using an extinction coefficient of 11.3 $mM^{-1}cm^{-1}$ at 450 nm. The anaerobic titration with NADPH was carried out by a procedure similar to the titration with dithionite. The concentration of NADPH was determined spectrophotometrically using an extinction coefficient of 6220 $M^{-1}cm^{-1}$ at 340 nm.

When studying the reductase chromophore at 402 nm, the enzyme was first fully reduced with NADPH or dithionite, and subsequently was exposed to air to become

reoxidized. The mixture was concentrated in an Amicon concentrator and washed several times with 60 mM KPi (pH 7.4). Both the concentrated enzyme and the filtrate were analyzed for enzyme activity and iron content.

RESULTS

The Impact of Enzyme Organization on Fatty Acid Oxidation

The plan was to specifically inhibit long-chain 3-ketoacyl-CoA thiolase and thereby the long-chain specific β-oxidation system in coupled mitochondria and to assess the functional consequence of this inactivation on fatty acid oxidation.

Synthesis and Evaluation of 4-Bromotiglic acid: A Potential Inhibitor of Fatty Acid β-oxidation

The most direct synthetic route to 4-bromotiglic acid is the bromination of tiglic acid or tiglic ester with *N*-bromosuccinimide. Since this approach yields an inseparable mixture of methyl 4-bromotiglate and methyl 2-bromomethylcrotonate (35), the desired product was synthesized from chloroacetaldehyde and (carb-*tert*-butoxyethylidene)triphenylphosphorane by a Wittig reaction (32). After the chloride was replaced with a bromine residue followed by acid hydrolysis of the ester, 4-bromotiglic acid was obtained in good yield.

When coupled rat liver mitochondria were preincubated with 10 μM 4-bromotiglic acid for 2 min, respiration supported by palmitoylcarnitine was completely inhibited (compare panels 1 and 4 of Figure 4). However, when mitochondria were first incubated with 2,4-dinitrophenol to uncouple respiration from oxidative phosphorylation,

4-bromotiglic acid was ineffective (see panels 2 and 5 of Figure 4). This observation supports the assumption that ATP is required for the activation of 4-bromotiglic acid, which thereafter may be further metabolized intramitochondrially to yield the activated inhibitor. When 2,4-dinitrophenol was added after 4-bromotiglic acid, palmitoylcarnitine-supported respiration remained completely inhibited (data not shown). An experiment with *n*-octanoate instead of palmitoylcarnitine as the respiratory substrate produced a different result. As is apparent from Figure 4, panels 3 and 6, octanoate-stimulated respiration initially was almost completely inhibited when mitochondria were pretreated with 4-bromotiglic acid. However, within 1 min, 90% of the original activity was recovered. This result demonstrated that the inhibition of octanoate-supported respiration is for the most part reversible. Moreover, octanoate, possibly by competing with 4-bromotiglic acid for mitochondrial activation or uptake, seems to prevent the further formation of the reversible inhibitor.

Since 4-bromotiglic acid caused the complete inhibition of palmitoylcarnitine-supported respiration, the target of the inhibitor might be one or several of the β-oxidation enzymes. To identify the site of the inhibition, coupled mitochondria were incubated with 4-bromotiglic acid and assayed for the enzymes of β-oxidation. As is apparent from the results shown in Table 1, only the thiolase activities were significantly reduced. The activity detected with acetoacetyl-CoA was inhibited to a greater extent than was the activity measured with the medium-chain substrate 3-ketooctanoyl-CoA. Since the inhibition of thiolases was detected after their extensive dilution by the assay medium, the inhibition seems to be irreversible. The loss of thiolase activity and the decrease of palmitoylcarnitine-supported respiration were functions of the inhibitor

concentration (see Figure 5A). The complete inhibition of respiration was achieved with 10 μM 4-bromotiglic acid after 2 min of incubation. At a fixed inhibitor concentration of 10 μM, the rate of respiration declined in a time-dependent manner (see Figure 5B). At all inhibitor concentrations, the decline of the thiolase activities was less severe than was the inhibition of respiration (see Figure 5A). The medium-chain thiolase activity was inhibited to a lesser extent than was acetoacetyl-CoA thiolase activity. This observation is indicative of a differential inactivation of the various thiolases present in mitochondria.

Rat liver mitochondria contain at least three types of thiolase. They are acetoacetyl-CoA thiolase, which only acts on acetoacetyl-CoA thiolase, 3-ketoacyl-CoA thiolase with a broad chain length specificity, and long-chain 3-ketoacyl-CoA thiolase, which acts on all substrates except for acetoacetyl-CoA (1). For determining the effects of 4-bromotiglic acid on the individual thiolases, mitochondria were treated with 30 μM 4-bromotiglic acid for 3 min, sonicated, and subjected to fractionation on DEAE-cellulose. Acetoacetyl-CoA thiolase and 3-ketoacyl-CoA thiolase, both of which are soluble matrix enzymes, did not bind to the column and emerged in the forerun (see Figure 6, panels A and B). Long-chain 3-ketoacyl-CoA thiolase, which is a protein of the inner mitochondrial membrane, was retained by the column and was eluted with a KCl gradient (see Figure 6, panels C and D). A comparison of the control (Figure 6, panels A and C) with the inhibitor-treated sample (Figure 6, panels B and D) demonstrated the complete inactivation of long-chain 3-ketoacyl-CoA thiolase (Figure 6, panel D) while a fraction of the 3-ketoacyl-CoA thiolase (approximately 15%) was still active. Separation of acetoacetyl-CoA thiolase and 3-ketoacyl-CoA thiolase by chromatography on phosphocellulose revealed the complete inactivation of the former enzyme, whereas a

fraction of the latter thiolase remained active (data not shown). Since acetoacetyl-CoA thiolase is not involved in fatty acid oxidation (1), 3-ketoacyl-CoA thiolase is assumed to be the only thiolase responsible for the degradation of medium-chain and short-chain fatty acids.

Probing Mitochondrial β-Oxidation with 4-Bromotiglic Acid

The cooperation between the two mitochondrial β-oxidation systems was evaluated by using 4-bromotiglic acid to completely inactivate long-chain 3-ketoacyl-CoA thiolase while retaining part of the 3-ketoacyl-CoA thiolase activity. For this purpose, mitochondria were preincubated for 2 min with various concentrations of 4-bromotiglic acid. The remaining capacity to oxidize fatty acids was then analyzed by measuring respiration supported by several substrates of β-oxidation. Respiration measurements were carried out in the presence and absence of the inhibitor to distinguish between irreversible and reversible modes of inhibition. The assumption was that the reversible inhibition would only persist if the inhibitor was present in the incubation medium. With palmitoylcarnitine as the substrate, the rate of respiration declined almost linearly as the inhibitor concentration was raised from 0 to 10 μM (see Figure 7A). The same results were obtained whether or not the inhibitor was present during the respiration measurements. However, with octanoylcarnitine as the substrate, the degree of the inhibition was greatly reduced when 4-bromotiglic acid was removed from the incubation medium before the respiration was measured (see Figure 7C). A possible explanation of these different results is that palmitoylcarnitine was first acted upon by the long-chain β-oxidation system which was completely inactivated. In contrast, octanoylcarnitine is a

substrate of the medium-chain/short-chain system that remained partially active. The results obtained with octanoic acid as the substrate (see Figure 7D) confirm this interpretation even though the inhibition is generally less severe than is the inhibition of octanoylcarnitine-supported respiration (compare the inhibitor concentrations in Figure 7, panels C and D). Surprisingly, the removal of the inhibitor did not relieve the inhibition observed with 2-methyldecanoic acid as the respiratory substrate. This result is attributed to the complete inhibition of long-chain 3-ketoacyl-CoA thiolase which, in contrast to the matrix 3-ketoacyl-CoA thiolase, is active with 2-methyl branched substrates (51). It seems that 3-ketoacyl-CoA thiolase and thereby the β-oxidation system present in the mitochondrial matrix system remained partially active while the long-chain system was completely inactivated. This situation provided the opportunity for determining the capacity of the matrix system to degrade fatty acids of various chain lengths. As is apparent from Figure 8, 10 μM 4-bromotiglic acid caused the complete inhibition of respiration supported by any of the tested acylcarnitines from octanoylcarnitine to palmitoylcarnitine (Figure 8). However, when the inhibitor was removed from the incubation medium before the respiration was measured, complete inhibition was only observed with palmitoylcarnitine as the substrate. Shorter-chain substrates did support residual rates of respiration. A clear trend was detectable, with the remaining relative respiration increasing from 0% to almost 70% as the acyl chain length decreased from 16 to 8 carbon atoms (see Figure 8). Interestingly, even a presumed long-chain substrate like myristoylcarnitine sustained roughly 25% of the optimal respiration rate in mitochondria with a long-chain β-oxidation system that was completely inactive toward palmitoylcarnitine.

Oxidation of Conjugated Polyunsaturated Fatty Acids

Metabolism of 5,7-Decadienoyl-CoA

The β-oxidation of polyunsaturated fatty acids with odd-numbered conjugated double bonds is expected to generate 5,7-dienoyl-CoA intermediates. To study the metabolism of these intermediates, 5,7-decadienoyl-CoA was synthesized. The required 5,7-decadienoic acid was prepared from (4-carboxybutylidene)triphenylphosphorane and 2-*trans*-pentenal by a Wittig reaction (36). Since the synthetic procedure is predicted to yield mostly the *trans* isomer of the newly formed double bond, the major product is expected to be 5-*trans*,7-*trans*-decadienoic acid. The CoA derivative of this acid was obtained in pure form after converting the acid to the CoA thioester and isolating the major product by HPLC (see Fig. 9A).

In a preliminary experiment, the capacity of mitochondria to degrade fatty acids with odd-numbered conjugated double bonds was assessed. The data presented in Table II demonstrate that such fatty acids support the respiration of coupled rat liver mitochondria although at rates that were slightly lower than those obtained with the corresponding fatty acids having either non-conjugated double bonds or no double bond at all. This result suggests the presence of a mitochondrial pathway for the β-oxidation of fatty acids with odd-numbered conjugated double bonds.

The step-by-step degradation of 5,7-decadienoyl-CoA was studied spectrophotometrically by use of purified enzymes. The spectrum of 5,7-decadienoyl-CoA, shown in Fig. 10A, curve 1, is characterized by a major absorbance band centered around 230 nm and a shoulder at 260 nm. These absorbances are attributed to the diene

and CoA chromophore, respectively. Treatment of 5,7-decadienoyl-CoA with acyl-CoA oxidase produced a 40% increase in the absorbance at 263 nm (see Fig. 10A). Such change in absorbance agrees with the conversion of an acyl-CoA to 2-*trans*-enoyl-CoA. 5,7-Decadienoyl-CoA is also a substrate of medium-chain acyl-CoA dehydrogenase. In fact, it is a better substrate than decanoyl-CoA (0.66 *vs.* 0.46 units/mg). When the product, presumed to be 2,5,7-decatrienoyl-CoA, was treated with Δ^3,Δ^2-enoyl-CoA isomerase, the absorbance at 260 nm increased while the absorbance around 230 nm decreased (see Fig. 10A). These absorbance changes agree with the isomerization of a conjugated diene to a conjugated triene that would take place during the conversion of 2,5,7-decatrienoyl-CoA to 3,5,7-decatrienoyl-CoA. The same absorbance changes were observed when 5,7-decadienoyl-CoA was reacted with acyl-CoA oxidase and the multifunctional protein I which harbors Δ^3,Δ^2-enoyl-CoA isomerase activity (see Fig. 10B).

When the suspected 3,5,7-decatrienoyl-CoA was treated with a soluble extract of rat liver mitochondria or a partially purified preparation of dienoyl-CoA isomerase, an absorbance band close to 340 nm appeared, while the absorbance at 260 nm declined (see Fig. 10C). The increase in the absorbance at 340 nm agrees with the formation of a 2,4,6-trienoyl-CoA, which was reported to have an absorbance maximum at 337 nm (12). Since 2,4,6-octatrienoyl-CoA was found to be reduced by NADPH-dependent 2,4-dienoyl-CoA reductase (12), this reaction was used to confirm the structure of the suspected 2,4,6-decatrienoyl-CoA (Fig. 10C, spectrum 5 and 2D, spectrum 2). As shown in Fig. 10D, the chromophore at 340 nm disappeared in a time-dependent manner when

NAPDH and 2,4-dienoyl-CoA reductase were added to the buffered solution of 2,4,6-decatrienoyl-CoA.

Further evidence for the identity of 2,4,6-decatrienoyl-CoA was obtained by its enzymatic conversion and HPLC analysis of the resultant products. For this purpose, synthetic 5,7-decadienoyl-CoA (Fig. 9A) was converted to 3,5,7-decatrienoyl-CoA by acyl-CoA oxidase and the peroxisomal multifunctional protein I. The resultant two compounds (see Fig. 9B) are assumed to be the 3-*cis* (minor peak) and 3-*trans* isomers (major peak) of 3,5,7-decatrienoyl-CoA because both are converted to 2,4,6-decatrienoyl-CoA by a partially purified preparation of dienoyl-CoA isomerase (see Fig. 9C). The reduction of 2,4,6-decadienoyl-CoA (Fig. 9D) by NADPH in the presence of 2,4-dienoyl-CoA reductase yielded a single product that was eluted at the same position as was the starting material (compare panels D and E of Fig. 9). However, the addition of crotonase to the reaction product, presumed to be 2,6-decadienoyl-CoA, produced a more polar compound, most likely 3-hydroxydec-6-enoyl-CoA (see Fig. 9F). In contrast, the addition of crotonase to 2,4,6-decatrienoyl-CoA (Fig. 9D) did not produce a product of different polarity. This experiment supports the assigned structures of 2,4,6-decatrienoyl-CoA (Fig. 9D) and 2,6-decadienoyl-CoA (Fig. 9E) because 2-enoyl-CoA compounds are only hydrated to a significant extent when the 2-double bond is conjugated only with the thioester but not when it is part of a more extended chromophore (29).

Although 5,7-decadienoyl-CoA can be converted to 2,4,6-decatrienoyl-CoA and further degraded after the NADPH-dependent reduction of the latter intermediate, the operation of this pathway in mitochondria had not been demonstrated. Toward this end, the metabolism of 2,5,7-decatrienoyl-CoA by a soluble extract of rat liver mitochondria

was investigated. Rates of the direct β-oxidation of 2,5,7-decatrienoyl-CoA in the presence of CoASH and NAD^+ were determined by measuring the formation of NADH fluorometrically (see Fig. 11A). These rates were compared with rates of 2,4,6-decatrienoyl-CoA formation that had been determined in the presence of excess trienoyl-CoA isomerase but in the absence of cofactors (see Fig. 11B). The direct β-oxidation was found to be the favored pathway (see Fig. 11). However, the degradation of 2,5,7-decatrienoyl-CoA via 2,4,6-decatrienoyl-CoA makes a significant contribution to the total metabolism of 2,5,7-decatrienoyl-CoA accounting for almost 50% of the total flux at low and high substrate concentrations.

Identification and Characterization of $\Delta^{3,5,7},\Delta^{2,4,6}$-Trienoyl-CoA Isomerase from Pig Heart

The identification of $\Delta^{3,5,7},\Delta^{2,4,6}$-trienoyl-CoA isomerase prompted its further characterization and purification. Since a partially purified preparation of dienoyl-CoA isomerase exhibited trienoyl-CoA isomerase activity, the relationship between these two enzymatic activities was evaluated by an immunoprecipitation experiment. As is apparent from Fig. 12, the trienoyl-CoA activity was precipitated by antibodies raised against dienoyl-CoA isomerase. The two immunoprecipitation curves were close enough to suspect that the two enzymes might be associated with the same protein.

The relationship between trienoyl-CoA isomerase and dienoyl-CoA isomerase was further investigated by studying their behaviors during purification from pig heart. The enzymes were purified from heart to reduce a possible interference by peroxisomal forms of these enzymes. The results of this purification effort, summarized in Table III,

demonstrate the co-purification of these two enzymes. The activities of trienoyl-CoA and dienoyl-CoA isomerase remained inseparable throughout the procedure even though DI:TI ratio changed from 35:1 to 143:1. The result of the last purification step, the elution of the purified enzyme from a Reactive Red 120 column, is shown in Fig. 13A. The elution of trienoyl-CoA isomerase from this column coincided with the appearance of dienoyl-CoA isomerase and was proportional to the amount of protein present in each fraction. Moreover, an analysis of individual column fractions by SDS-PAGE revealed the presence of only one band (see Fig. 13B) that corresponded to a protein with a molecular mass close to 32 Kda which is the mass reported for dienoyl-CoA isomerase.

2,4-Dienoyl-CoA Reductase from *E. coli*

2,4-Dienoyl-CoA Reductase from E. coli Does Not Have cis-trans Isomerase, nor Δ^3,Δ^2-Enoyl-CoA Isomerase Activities

Since bovine liver and *E. coli* 2,4-dienoyl-CoA reductases effectively catalyze the reductions of both 2-*trans*,4-*cis*- and 2-*trans*,4-*trans*-dienoyl-CoAs, it is possible that both bovine liver and *E. coli* reductase have *cis-trans*-isomerase activity. Since 2-*trans*,4-*trans*-decadienoyl-CoA is thermodynamically more stable, the reductases probably would convert 2-*trans*,4-*cis*-decadienoyl-CoA to 2-*trans*,4-*trans*-decadienoyl-CoA. Various amounts of 2,4-dienoyl-CoA reductase from *E. coli* were incubated with 2-*trans*,4-*cis*-decadienoyl-CoA for 30 sec in the absence of NADPH before the reductase was removed by acidification. The formation of 2-*trans*,4-*trans*-decadienoyl-CoA was monitored by HPLC. As shown in Figure 15 (panel A, B, and C), there was no indication of the formation of 2-*trans*,4-*trans*-decadienoyl-CoA.

In bovine liver, 2,4-dienoyl-CoA is reduced to 3-*trans*-enoyl-CoA which in turn is isomerized to 2-*trans*-enoyl-CoA by Δ^3,Δ^2-enoyl-CoA isomerase. On the other hand, in *E. coli*, 2-*trans*-enoyl-CoA is the reduction product. Assuming that the reductases from both bovine liver and *E. coli* catalyze the reduction of 2,4-dienoyl-CoA by a similar mechanism, 2,4-dienoyl-CoA reductase from *E. coli* might have an endogenous Δ^3,Δ^2-enoyl-CoA isomerase activity that would be responsible for the conversion of 3-enoyl-CoA intermediates to 2-enoyl-CoA products. To test this hypothesis, *E. coli* 2,4-dienoyl-CoA reductase was incubated with 3-*trans*-decenoyl-CoA in the presence 0.42 mU of crotonase (Fig. 15, panel F) for 3 min. However, neither 3-hydroxydecanoyl-CoA nor Δ^2-decenoyl-CoA was detected. The products of the reduction of 2-*trans*,4-*cis*-decadienoyl-CoA catalyzed by *E. coli* reductase in the absence or in the presence of crotonase, respectively served as controls to aid in the identification of 2-*trans*-decenoyl-CoA and 3-hydroxydecanoyl-CoA (Fig. 15, panels D and E).

UV-VIS Spectroscopy of 5-Phenyl-2,4-pentadienoyl-CoA Bound to 2,4-Dienoyl-CoA Reductase from E. coli

Large UV-VIS red shifts had been observed for 4-(N, N-dimethylamino)cinnamoyl-CoA bound to crotonase (52) and for 4-(N, N-dimethylamino)cinnamaldehyde complexed with alcohol dehydrogenase (53) or aldehyde dehydrogenase (54). These observations prompted the idea that 5-phenyl-2,4-pentadienoyl-CoA might exhibit a significant UV-VIS red shift upon binding to *E. coli* 2,4-dienoyl-CoA reductase. 5-Phenyl-2,4-pentadienoyl-CoA was incubated with an excess molar amount of *E. coli* 2,4-dienoyl-CoA reductase. The spectrum of bound 5-

phenyl-2,4-pentadienoyl-CoA was obtained by subtracting the spectrum of *E. coli* reductase from that of the *E. coli* reductase 5-phenyl-2,4-pentadienoyl-CoA complex. The results indicate that the spectrum of 5-phenyl-2,4-pentadienoyl-CoA upon binding to the reductase (Fig. 16, curve 2) is red shifted by 38 nm (Fig. 16, curve 1).

E. coli 2,4-Dienoyl-CoA Reductase is a Novel Iron-Sulfur Flavoprotein

The UV-visible spectrum of purified *E. coli* 2,4-dienoyl-CoA reductase (Fig. 17, curve 1) showed absorbance maxima at 480, 450, 402, and 380 nm that are typical of iron-sulfur flavoprotein. The extinction coefficient at 450 nm was calculated to be 34.4 $mM^{-1}cm^{-1}$. The absorbance at 450 nm in the spectrum of the denatured enzyme (Figure 17, curve 2) was approximately the same as that in the spectrum of an equimolar mixture of free FAD and FMN (Figure 17, curve 3).

The flavins, which were released from *E. coli* reductase upon the acidic denaturation of the enzyme, were analyzed by HPLC. Dommes and Kunau (13) reported that *E. coli* 2,4-dienoyl-CoA reductase contained 1 mole of FAD per mole of enzyme. Besides detecting a peak corresponding to FAD, an additional peak was observed that was suspected to be FMN (Figure 18, panel B). The HPLC pattern of an equimolar mixture of free FAD and FMN was almost identical with the pattern of peaks due to cofactors released from the *E. coli* reductase (compare panel A and B in Fig. 18). In order to identify FMN, the authentic flavins and the flavins released from the reductase were mixed and subjected to HPLC. As is apparent from Figure 18, panel C, the peaks corresponding to FAD and FMN were increased. This observation is indicative of the

presence of both FAD and FMN in *E. coli* reductase. Free FAD was stable in 10% TCA under the experimental conditions used in this experiment (data not shown).

The contents of FAD and FMN released from the *E. coli* reductase were determined from the area under the peaks with purified FAD and FMN as standards. As is apparent from Table IV, the molar ratio of either FAD or FMN to enzyme is close to 0.85. It seems that *E. coli* reductase contains 1 mole of FAD and 1 mole of FMN per mole of enzyme. FAD and FMN extracted from the reductase were also quantified fluorimetrically. Table IV shows that the molar ratio of either FAD to enzyme or FMN to enzyme is close to 1. Together, the evidence establishes that *E. coli* reductase indeed contains one mole of FAD and 1 mole of FMN per mole of enzyme.

Analysis of iron and sulfur revealed the presence of approximately four moles of iron and four moles of labile sulfur per mole of enzyme (Table IV). One possible conclusion is that one [4Fe-4S] cluster might be present in *E. coli* 2,4-dienoyl-CoA reductase. This possibility is consistent with a single CXXCXXXC motif in the amino acid sequence of the *E. coli* reductase.

Anaerobic Reduction of Oxidized Enzyme

The results of the spectrophotometric titration of oxidized 2,4-dienoyl-CoA reductase with sodium dithionite under anaerobic conditions are shown in Fig. 19A. An absorbance increase was observed at 380 nm during the early stage of the titration, while a sharp peak at 402 nm was detectable in partially reduced enzyme. These observations suggested the formation of red semiquinone. However, no evidence for a blue semiquinone was detected. It took approximately 7 moles of electrons per mole of

enzyme and several hours to completely reduce the oxidized enzyme. When the reduced enzyme was subsequently exposed to air, it was reoxidized. As is apparent from Fig. 20, the absorbance at 450 nm was fully recovered. However, the absorbance at 380 nm was only partially recovered and the chromophore at 402 nm was lost. These observations are not easily explained because the results shown in Table V indicate that this partially-reoxidized enzyme still exhibits full enzyme activity and contains the iron-sulfur cluster.

The results of the spectrophotometric titration of oxidized enzyme with NADPH under anaerobic conditions are shown in Fig. 19B. The spectral changes associated with the addition of aliquots of NADPH were different from those observed with the dithionite titration. It only took minutes and approximately 4.5 moles of electrons per mole of enzyme to fully reduce the enzyme. The absorbances at 380 nm, 402 nm, and 450 nm decreased simultaneously. No red or blue semiquinone was observed, neither was a charge transfer complex. When the reduced enzyme was subsequently either exposed to air or back-titrated with 2-*trans*,4-*trans*-decadienoyl-CoA, the recoveries of chromophores were similar to those observed with the dithionite titration (data not shown). Furthermore, when this partially reoxidized enzyme was re-titrated with NADPH under anaerobic conditions, absorbances of the two flavins at 380 nm and 450 nm were reduced (data not shown).

The results of the photoreduction of oxidized enzyme in the presence of EDTA and deazaflavin are shown in Fig. 19C. The spectral changes were different from either the dithionite titration or NADPH titration. Slight increases in absorbance at both 380 nm and 402 nm were observed early on, whereas a distinct peak at around 390 nm was observed during the middle stage of the titration. These observations suggested that a

relatively small amount of red semiquinone might be present during the photoreduction. No evidence for blue semiquinone was detected. An isosbestic point was apparent around 320 nm. The complete reduction of oxidized enzyme was obtained within 10 min of illumination. Compared with the spectra obtained after the dithionite or NADPH reduction, the photoreduced enzyme retained less absorbance at 450 nm.

Results of the back titration of photoreduced enzyme with ferricyanide is shown in Fig. 19D. The chromophores at 380 nm, 402 nm, and 450 nm were almost fully recovered. Back titration with ferricyanide is the best way to determine the stoichiometry of the electron uptake by the oxidized enzyme. Complete reoxidation of the fully reduced enzyme was observed upon the addition of 5 mole of ferricyanide per mole of enzyme.

Oxidation of *trans* Fatty Acids

Respirations Supported by Δ^6 or Δ^9-Octadecenoyl-CoAs in Coupled Rat Liver and Rat Heart Mitochondria

The first part of this study was designed to determine whether *cis*- and *trans*-octadecenoyl-CoA with an even-numbered or odd-numbered double bond are oxidized at different rates. Since long-chain fatty acid thioesters enter mitochondria via the carnitine-dependent uptake system (55), rates of respiration were measured with 15 μM of acyl-CoA in the presence of 0.5 mM L-carnitine. As is apparent from Fig. 21, in rat heart mitochondria the rate of respiration supported by elaidoyl-CoA was only about half of the rate sustained by oleoyl-CoA, whereas the rate of respiration supported by petroselaidoyl-CoA was only slightly lower than that supported by petroselinoyl-CoA. In

rat liver mitochondria, no significant differences between respiration rates were observed with stearoyl-CoA or the *cis*- and *trans*-isomers of Δ^6- and Δ^9-octadecenoyl-CoA (see Fig. 21).

Exploring the Oxidations of cis- and trans- Fatty Acids at the Molecular Level

In an attempt to explore the differences between the oxidations of *cis*- and *trans*-fatty acids in rat liver and rat heart mitochondria, stearoyl-CoA, oleoyl-CoA, elaidoyl-CoA, petroselinoyl-CoA, and petroselaidoyl-CoA were chosen as respiratory substrates. The incubation mixture for the respiration was scaled up ten times so that the metabolic intermediates could be detected by HPLC. Since the long-chain fatty acid thioester would precipitate and/or bind to some membrane proteins at low pH, the reaction was terminated with methanol instead of a strong acid at the indicated times.

When coupled rat liver mitochondria were incubated for 1 min with stearoyl-CoA, oleoyl-CoA, or elaidoyl-CoA, the metabolic intermediates derived from these acyl-CoAs were analyzed by HPLC. The results are shown in Figure 22. Although a metabolite, presumably hexanoyl-CoA, accumulated during the oxidation of all three fatty acyl-CoAs (Fig. 22, panels A, B, and C), significant differences between the patterns of metabolites derived from elaidoyl-CoA (Fig. 22, panel C), stearoyl-CoA (Fig. 22, panel A), and oleoyl-CoA (Fig. 22, panel B) were observed. The dominant long-chain metabolite derived from elaidoyl-CoA appeared to be 5-*trans*-tetradecenoyl-CoA, which was eluted at around 20 min (Fig. 22, panel C). Oleoyl-CoA yielded 5-*cis*-tetradecenoyl-CoA (Fig. 22, panel B) but at a much lower concentration while no evidence for the formation of tetradecanoyl-CoA form stearoyl-CoA was obtained. The pattern of metabolic intermediates derived from these acyl-CoAs in rat heart mitochondria was similar to that

observed with rat liver mitochondria (data not shown). Oxidation of petroselinoyl-CoA and petroselaidoyl-CoA in coupled rat liver and rat heart mitochondria was also examined. Although 4-*cis*-hexadecenoyl-CoA and 4-*trans*-hexadecenoyl-CoA derived from petroselinoyl-CoA and petroselaidoyl-CoA, respectively, accumulated, the intensity of 4-*trans*-hexadecenoyl-CoA was only slightly higher than that of 4-*cis*-hexadecenoyl-CoA (data not shown).

Since 5-*trans*-tetradecenoyl-CoA rapidly accumulated in both rat heart and rat liver mitochondria, it was of interest to determine the time course of its accumulation. Since the patterns of metabolic intermediates were similar in rat heart and rat liver mitochondria, time course studies of the oxidation of palmitoyl-CoA, stearoyl-CoA, oleoyl-CoA, and elaidoyl-CoA were carried out with rat liver mitochondria due to its greater availability. The intermediates were quantified using pentadecanoyl-CoA or nonanoyl-CoA as internal standards. The results are summarized in Fig. 23. The HPLC profiles of intermediates formed during the oxidation of elaidoyl-CoA at different reaction time points are also shown in Fig. 22, in panels D, E, and F. With all four respiratory substrates, the accumulation of hexanoyl-CoA and dodecanoyl-CoA was observed (Fig. 23, panels A, B, C, and D). The pattern of metabolic intermediates observed with stearoyl-CoA was quite different from that of palmitoyl-CoA. Although both yielded hexanoyl-CoA and dodecanoyl-CoA, only a small amount of tetradecanoyl-CoA was observed during the oxidation of stearoyl-CoA even during prolonged incubation (compared Fig. 23, panel A and B). The pattern of metabolic intermediates derived from oleoyl-CoA (Fig. 23, panel C) was different from that of stearoyl-CoA (Fig. 23, panel B). In addition to hexanoyl-CoA and dodecanoyl-CoA, 5-*cis*-tetradecenoyl-

CoA gradually accumulated. When the oxidation of elaidoyl-CoA (Fig. 23, panel D) was compared with that of oleoyl-CoA (Fig. 23, panel C), a much greater accumulation of 5-*trans*-tetradecenoyl-CoA than that of 5-*cis*-tetradecenoyl-CoA was noted. It seems that during the oxidation of elaidoyl-CoA the built up of hexanoyl-CoA and 5-*trans*-tetradecenoyl-CoA preceded that of dodecanoyl-CoA (Fig. 22, panels D, E, and F). On the other hand, during the oxidation of oleoyl-CoA the accumulation of hexanoyl-CoA and dodecanoyl-CoA preceded that of 5-*cis*-tetradecenoyl-CoA (Fig. 23, panel C).

Identification of Metabolic Intermediates

The HPLC fractions containing the metabolic intermediates, presumed to be hexanoyl-CoA, dodecanoyl-CoA, and 5-*trans*-tetradecenoyl-CoA, were collected, hydrolyzed under basic conditions, and then converted to their corresponding methyl esters before being applied to GC-MS. The identity of 5-*trans*-tetradecenoic acid methyl ester was confirmed by its GC-MS spectrum with a $(M + NH_4^+)$ peak at 258 (Fig. 24). The protonated molecular ion at 215 revealed the presence of dodecanoic acid methyl ester and the protonated molecular ion at 131 and $(M + NH_4^+)$ ion at 148 reflected the presence of hexanoic acid methyl ester (data not shown). Since the double bond position of tetradecenoyl-CoA could not be established by GC-MS, an enzymatic approach was chosen instead. The UV-VIS spectrum of the compound presumed to be 5-*trans*-tetradecenoyl-CoA is shown in Fig. 25, curve 1. When this compound was treated with acyl-CoA oxidase (Fig. 25, curve 2), the absorbance at 263 increased. Such change in absorbance agrees with the conversion of acyl-CoA to 2-*trans*-enoyl-CoA. When Δ^3,Δ^2-enoyl-CoA isomerase was added to the incubation mixture, the absorbance around 230

nm increased while the absorbance at 263 nm decreased (Fig. 23, curve 3). These absorbance changes agree with the formation of a conjugated diene that would take place during the conversion of 2,5-dienoyl-CoA to 3,5-dienoyl-CoA. When additionally $\Delta^{3,5},\Delta^{2,4}$-dienoyl-CoA isomerase was added to the incubation mixture, an absorbance band at 300 nm appeared while the absorbance at 230 declined. The increase in absorbance at 300 nm agrees with the formation of 2,4-dienoyl-CoA, which was reported to have an absorbance maximum at 300 nm (23).

Relative Activities of Various Acyl-CoA Dehydrogenases with Selected Substrates

The accumulation of the metabolic intermediates may reflect the chain-length specificities of different acyl-CoA dehydrogenases that control the degradation of these intermediates. The substrate specificities of several acyl-CoA dehydrogenases from rat liver were tested and are presented in Figure 26. Medium-chain acyl-CoA dehydrogenase is highly active with octanoyl-CoA but not with substrates having acyl chains with 14 or more carbon atoms. In contrast, long-chain acyl-CoA dehydrogenase is highly active with tetradecanoyl-CoA, hexadecanoyl-CoA, 5-*cis*-tetradecenoyl-CoA, and 5-*trans*-tetradecenoyl-CoA. Very long-chain acyl-CoA dehydrogenase on the other hand exhibits little activity with unsaturated tetradecenoyl-CoAs while being active with tetradecanoyl-CoA and hexadecanoyl-CoA.

DISCUSSION

The Impact of Enzymes Organization on Fatty Acid Oxidation

The first aim of this project was the design of an inhibitor that would irreversibly inactivate the long-chain specific system of fatty acid β-oxidation located in the inner mitochondrial membrane. Of the four enzymes that constitute the long-chain β-oxidation system, namely very long-chain acyl-CoA dehydrogenase, long-chain enoyl-CoA hydratase, long-chain 3-hydroxyacyl-CoA dehydrogenas, and long-chain 3-ketoacyl-CoA thiolase, thiolase is most amenable to chemical inactivation owing to its essential sulfhydryl group. A number of thiolase inhibitors have been designed and tested (56). A very effective one is 4-bromocrotonic acid which is metabolized in coupled mitochondria to 3-keto-4-bromobutyryl-CoA (40). This metabolite inactivates acetoacetyl-CoA thiolase (40), 3-ketoacyl-CoA thiolase (40), and long-chain 3-ketoacyl-CoA thiolase (Cheng, H., and Schulz, H., unpublished observation). The plan was to design a derivative of 4-bromocrotonic acid that would inactivate the long-chain thiolase but not 3-ketoacyl-CoA thiolase. The effect of the inhibitor on acetoacetyl-CoA thiolase would be inconsequential because acetoacetyl-CoA thiolase is not involved in fatty acid β-oxidation (1). 4-Bromocrotonic acid with a 2-methyl substituent (4-bromotiglic acid) was a potential inhibitor of long-chain thiolase because it was expected to be metabolized intramitochondrially to 3-keto-4-bromo-2-methylbutyryl-CoA which is a likely substrate of long-chain 3-ketoacyl-CoA thiolase but not of 3-ketoacyl-CoA thiolase (51). Since the inhibition of thiolases by this group of inhibitors is assumed to be mechanism-based (56), the preferential inactivation of 3-ketoacyl-CoA thiolase was predicted.

The observed inhibition of palmitoylcarnitine-supported respiration by 4-bromotiglic acid in the absence of a severe effect on octanonoate-driven respiration agrees with the expected inactivation of the long-chain β-oxidation system by this

compound without having a serious effect on the medium-chain/short-chain β-oxidation system. In addition, this result proves that the inhibitor does not affect reactions downstream of β-oxidation. The anti-inhibitory effect of 2,4-dinitrophenol in mitochondria incubated with 4-bromotiglic acid was most likely due to the abolishment of ATP synthesis and the resultant failure of 4-bromotiglic acid to undergo activation to its CoA thioester. The same observation had been made with 4-bromocrotonic acid and 4-bromo-2-octenoic acid (40,57) which additionally underwent partial β-oxidation before becoming inhibitors of thiolases and thereby of β-oxidation. Similarly, 4-bromotigloyl-CoA is assumed to be hydrated and dehydrogenated, presumably by enoyl-CoA hydratase (crotonase) and short-chain 3-hydroxy-2-methylacyl-CoA dehydrogenase, respectively (51), to yield 3-keto-4-bromo-2-methylbutyryl-CoA which may be the actual inhibitor of thiolases. The inactivation of all three known thiolases by 4-bromotiglic acid, in the absence of significant effects on other enzymes of β-oxidation, was demonstrated. However, long-chain 3-ketoacyl-CoA and acetoacetyl-CoA thiolase were inactivated more severely than was 3-ketoacyl-CoA thiolase. In addition to being irreversibly inhibited, the thiolases also were reversibly inhibited. However, the reversible inhibition persisted only as long as 4-bromotiglic acid was present in the incubation mixture and was continuously metabolized intramitochondrially. Competition of octanoic acid and 4-bromotiglic acid for activation by medium-chain acyl-CoA synthetase or, less likely, competition for uptake relieved the reversible inhibition as did the removal of the inhibitor from the incubation medium. This observation supports the notion that the compound responsible for the reversible inhibition, possibly 4-bromo-3-keto-2-methylbutyryl-CoA, is short-lived due to its instability or further metabolism. Once the

reversible inhibition was abolished, medium-chain substrates such as octanoylcarnitine and octanoate, in contrast to the long-chain substrate palmitoylcarnitine, were oxidized. The only exception was the medium-chain substrate 2-methyldecanoic acid which did not serve as a respiratory substrate, presumably because it is acted upon only by long-chain 3-ketoacyl-CoA thiolase but not by 3-ketoacyl-CoA thiolase (51). This interpretation agrees with the observation that long-chain 3-ketoacyl-CoA thiolase was totally inactivated while 3-ketoacyl-CoA thiolase retained part of its activity.

The differential inactivation of the two thiolases permitted an evaluation of their functions in the β-oxidation of fatty acids with different chain lengths. The use of acylcarnitines assured that all substrates entered mitochondria via the same uptake system. However, both carnitine palmitoyltransferase II and carnitine acetyltransferase may be required for the intramitochondrial acyl transfers from carnitine to CoASH. With palmitoylcarnitine as the substrate no respiration was detected, whereas shorter-chain substrates exhibited residual activities that increased with decreasing acyl chain length. Since the matrix 3-ketoacyl-CoA thiolase is highly active with all 3-ketoacyl-CoA intermediates formed during the β-oxidation of palmitate (58), the chain length specificity of the residual β-oxidation capacity is not explained by the remaining thiolase activity. The results fit a model based on the assumption that palmitoyl-CoA must be chain shortened by the membrane-bound β-oxidation system, whereas shorter-chain substrates can be degraded, at least in part, by the β-oxidation system in the matrix. The degradation of dodecanoyl-CoA and shorter-chain substrates seems to be affected only slightly by the inactivation of the long-chain β-oxidation system.

In conclusion, it seems that palmitoyl-CoA and most likely longer-chain acyl-CoA thioesters are obligatory substrates of the long-chain β-oxidation system. Moreover, it appears that the inactivation of one component enzyme of this β-oxidation system, for example, long-chain 3-ketoacyl-CoA thiolase, leaves the whole system inactive. This finding agrees with the reported intermediate channeling on the trifunctional β-oxidation enzyme (5), which catalyzes three of the four reactions of the long-chain β-oxidation system. Altogether, the observations fit a model of two mitochondrial β-oxidation systems cooperating in the degradation of long-chain fatty acids. The main transfer of intermediates between the two systems seems to occur after the completion of one or several full cycles of β-oxidation when the length of the acyl chain has been reduced to 14 or 12 carbon atoms.

Oxidation of Polyunsaturated Fatty Acids

The observation that the CoA derivatives of fatty acids with two conjugated double bonds at odd-numbered positions, e.g. 9-*cis*,11-*trans*-octadecadienoyl-CoA (see Fig. 14, compound I), sustain mitochondrial respiration demonstrated their degradation by mitochondrial β-oxidation. Chain shortening of such unsaturated fatty acyl-CoAs by β-oxidation is expected to produce 5,7-dienoyl-CoA intermediates (Fig. 14, compound II). Based on evidence obtained with monounsaturated fatty acids that have a double bond at an odd-numbered position (23), the degradation of 5,7-dienoyl-CoA is predicted to proceed by two different routes. Common to both of them would be the dehydrogenation of 5,7-dienoyl-CoA to 2,5,7-trienoyl-CoA (see Fig. 14, compound III) catalyzed by one of the acyl-CoA dehydrogenases. If 2,5,7-trienoyl-CoA completes the

cycle of β-oxidation, the resultant product would be 3,5-dienoyl-CoA. The further metabolism of such an intermediate has been shown to require the sequential actions of dienoyl-CoA isomerase, 2,4-dienoyl-CoA reductase, and enoyl-CoA isomerase to produce 2-*trans*-enoyl-CoA which can re-enter the β-oxidation spiral (23). If however, enoyl-CoA isomerase catalyzes the isomerization of the double bond from the 2,3-position to 3,4-position, 3,5,7-trienoyl-CoA (see compound IV in Fig. 14) would be formed. The evidence presented in this report indicates that a significant fraction of the 2,5,7-trienoyl-CoA is converted to the 3,5,7-isomer even though the major portion of 2,5,7-trienoyl-CoA completes the cycle of β-oxidation and thereby bypasses the formation of a trienoyl-CoA intermediate. The further metabolism of 3,5,7-trienoyl-CoA was unknown hitherto. The identification of $\Delta^{3,5,7}$,$\Delta^{2,4,6}$-trienoyl-CoA isomerase suggested a pathway for the complete degradation of 3,5,7-trienoyl-CoAs. Isomerization of 3,5,7-trienoyl-CoA by trienoyl-CoA isomerase would yield 2,4,6-trienoyl-CoA (Fig. 14, compound V) which can be reduced to 3,6-dienoyl-CoA by NADPH-dependent 2,4-dienoyl-CoA reductase (12). The complete degradation of the latter intermediate would proceed by well established reactions that require the action of enoyl-CoA isomerase to shift the odd-numbered double bond from carbon 3 to 2 and 2,4-dienoyl-CoA reductase and enoyl-CoA isomerase to reductively remove the even-numbered double bond.

The co-purification of trienoyl-CoA isomerase and dienoyl-CoA isomerase as well as the co-immunoprecipitation of these two enzyme activities by antibodies raised against dienoyl-CoA isomerase strongly suggested that both enzymes reside on one protein. The demonstration that one protein, as indicated by a single band on SDS-PAGE, exhibited both trienoyl-CoA isomerase and dienoyl-CoA isomerase activities

confirmed the conclusion about the association of both enzyme activities with one protein.

Dienoyl-CoA isomerase was first isolated from rat liver mitochondria and reported to have a subunit molecular mass of 32 Kda (11). Subsequently, peroxisomes were shown to contain a form of this enzyme that cross-reacted with antibodies raised against the mitochondrial enzyme (59). The molecular cloning of dienoyl-CoA isomerase yielded a cDNA sequence that strongly suggested a peroxisomal as well as mitochondrial localization of this protein (60). Evidence in support of the dual subcellular localization of this protein was obtained by immunoelectron microscopy. However, the amino-terminal sequences of the mature forms of dienoyl-CoA isomerase detected in mitochondria and peroxisomes have not been reported.

Since the published cDNA sequence encodes a 36-Kda polypeptide, molecular masses of greater than 36 Kda reported for this enzyme (60,61) must be those of other polypeptides. Finally, expression of a fragment of the cDNA coding for dienoyl-CoA isomerase yielded an active protein that was crystallized and analyzed by X-ray diffraction (62). The crystal structure revealed an active site pocket that is hydrophobic except for the side chain of three acidic residues. Two of these residues, Glu 196 and Asp 204, were proposed to facilitate the proton removal from carbon 2 and the proton addition to carbon 6, respectively, of the substrate, 3,5-dienoyl-CoA. If 3,5,7-trienoyl-CoA binds to the same active site, the proton abstraction from carbon 2 could also be facilitated by Glu 196. However, the residue involved in the protonation of carbon 8 remains to be identified.

2, 4-Dienoyl-CoA Reductase from *E. coli*

Since both bovine liver reductase and *E. coli* reductase effectively catalyze the reduction of 2-*trans*,4-*cis*-decadienoyl-CoA and 2-*trans*,4-*trans*-decadienoyl-CoA (13), it was suspected that the reductase might harbor a *cis-trans* isomerase activity which would convert 2-*trans*,4-*cis*-decadienoyl-CoA to 2-*trans*,4-*trans*-decadienoyl-CoA. In bovine liver, the reduction product is 3-*trans*-decenoyl-CoA, which is further isomerized to 2-*trans*-decenoyl-CoA by Δ^3,Δ^2-enoyl-CoA isomerase. In contrast, in *E. coli* 2-*trans*-decenoyl-CoA is the reduction product. Therefore it is possible that the *E. coli* reductase might have an Δ^3,Δ^2-enoyl-CoA isomerase activity which would convert the initial reduction product, 3-*trans*-decenoyl-CoA, to 2-*trans*-decenoyl-CoA. But the results obtained in this study demonstrate that *E. coli* 2,4-dienoyl-CoA reductase does not have a *cis-trans* isomerase activity, nor a Δ^3,Δ^2-enoyl-CoA isomerase activity. The absence of the two hypothetical isomerase activities suggests that the reduction mechanism of bovine liver reductase is different from that of *E. coli* reductase. With bovine liver reductase the hydride transferred from NADPH to carbon 5 of the substrate while carbon 2 accepts a proton from a reductase residue functioning as a general acid. In contrast, the *E. coli* reductase catalyzes a hydride transfer from NADPH to the flavin moieties. The electrons are presumed to flow from FAD, to Fe-S center, and to FMN before they reach carbon 5 of the substrate. Carbon 4 subsequently or simultaneously accepts a proton from the solvent or from a reductase residue that functions as a general acid. Therefore it is not surprising that Dommes and Kunau detected tritium in the solvent instead of the product when they used 4S-[4-^{3}H] NADPH as coenzyme of the *E. coli* reductase (13).

Because of mechanistic and structural differences between mammalian reductase and *E. coli* reductase (14), it is likely that their reduction mechanisms are different.

The UV-VIS spectrum of 5-phenyl-2,4-pentadienoyl-CoA was significantly red-shifted upon binding to *E. coli* 2,4-dienoyl-CoA reductase. D'Ordine et al. (52) have observed a significant red shift upon cinnamoyl-CoA binding to crotonase. By analyzing the Raman spectra of free and crotonase-bound 2-*trans*,4-*trans*-hexadienoyl-CoA, Carey and Tonge (63) demonstrated that crotonase induced a conformational change in 2-*trans*,4-*trans*-hexadienoyl-CoA that caused a strong electron polarization of the –C=C-C(=O)- bonds. Assuming that similar changes occur when 5-phenyl-2,4-pentadienoyl-CoA binds to the reductase, it is likely that there is an increase in the electron density at the oxygen atom and a decrease of electron density at carbon 5. The phenyl group may contribute to the stabilization of the partial positive charge at carbon atom 5. But the main stabilization of the enzyme-bound substrate must be provided by the *E. coli* reductase. In keto steroid isomerase, Austin et al. proposed that the polarization of the substrate was largely due to a tyrosine forming a H-bond with the carbonyl oxygen and the carboxylate of the general base responsible for proton abstraction (64).

The absorption spectrum of native *E. coli* reductase has features similar to those seen with other Fe-S flavoproteins. The spectrum of the denatured reductase in guanidine hydrochloride suggests that the enzyme might contain two flavins in addition to a group responsible for the chromophore at 402 nm. Analysis of the flavins, which were released from *E. coli* reductase with 10% TCA and separated by HPLC, clearly indicates that *E. coli* reductase contains equal amounts of FAD and FMN. Fluorimetric analysis further confirms that *E. coli* reductase harbors 1 mole of FAD and 1 mole of FMN per mole of

enzyme. Iron and labile sulfur analyses suggest that the enzyme possibly contains a single [4Fe-4S] cluster per enzyme molecule. This notion agrees with the presence of a single CXXCXXXC motif in the amino acid sequence of *E. coli* reductase. Thus *E. coli* reductase belongs to the rare class of iron-sulfur flavoproteins. One member of this class of enzyme is enoate reductase from *Clostridium tyrobutyricum* which contains FAD, FMN and a [4Fe-4S] cluster and which exhibits a 30% amino acid homology with dienoyl-CoA reductase (65,66).

The ability of the *E. coli* reductase to accept electrons from reducing agents is relevant to its function in biological systems. *E. coli* reductase can be reduced by dithionite and NADPH anaerobically and can undergo photoreduction. Both NADPH reduction and photoreduction proceed more rapidly than dithionite reduction. Neither a blue semiquinone nor a charge transfer complex was detected in all three types of reductions. But some evidence for the formation of a red semiquinone was obtained during the dithionite reduction and photoreduction. Massey and Hemmerich reported that red semiquinone rather than blue semiquinone was observed during the photoreduction of *old yellow* enzyme (48). *E. coli* reductase requires approximately 5 electrons for its full reduction. The chromophore at 402 nm was lost when the enzyme after its reduction by dithionite or NADPH was exposed to air. However, the absorbance was mostly retained when the photoreduced enzyme was back-titrated with ferricyanide. This observation suggests that the recovery of the 402 nm chromophore depends on the nature of reductant or oxidant. Although the chromophore at 402 nm was lost after the native enzyme was reduced and reoxidized by air, the partially reoxidized enzyme still exhibited full enzyme activity and retained the iron-sulfur center. This phenomenon remains unexplained. It

would also be very interesting to know how the electrons flow from NADPH to the two flavins and to the Fe-S center.

Oxidation of *trans* Fatty Acids

The rate of respiration supported by elaidoyl-CoA in rat heart mitochondria was approximately half of that observed with stearoyl-CoA or oleoyl-CoA. In contrast, in rat liver mitochondria, the rates of respiration supported by either stearoyl-CoA, oleoyl-CoA or elaidoyl-CoA were almost the same. Willebrands and Van Der Veen have reported that 5-*trans*-tetradecenoic acid, but not 5-*cis*-tetradecenoic acid, accumulated in the perfusion medium when they studied the oxidation of elaidic acid and oleic acid in the perfused rat heart (67). In an attempt to explore the differences between the oxidations of *cis* and *trans* fatty acids, isolated rat heart or rat liver mitochondria were incubated with either stearoyl-CoA, oleoyl-CoA or elaidoyl-CoA under the conditions used to measure rates of respiration. Metabolic intermediates, derived from these acyl-CoAs, were analyzed by HPLC. 5-*trans*-Tetradecenoyl-CoA, which is derived from elaidoyl-CoA, was observed to accumulate in both isolated rat liver and rat heart mitochondria. In rat liver mitochondria the amount of 5-*trans*-tetradecenoyl-CoA that accumulated was approximately three-fold higher than that of the corresponding 5-*cis*-tetradecenoyl-CoA which is derived from oleoyl-CoA. On the other hand, in rat heart mitochondria the amount of accumulated 5-*trans*-tetradecenoyl-CoA was only two-fold higher than that of the corresponding 5-*cis*-tetradecenoyl-CoA (data not shown). Presumably elaidoyl-CoA was oxidized at only half of the rate at which oleoyl-CoA was oxidized.

It is not quite clear why 5-*trans*-tetradecenoyl-CoA accumulated in such considerable amounts. The β-oxidation is apparently inhibited after two cycles of the fatty acid oxidation spiral. One could speculate that the dehydrogenation by acyl-CoA dehydrogenases might proceed at a slower rate with 5-*trans*-acyl-CoA because of steric hindrance. Long-chain acyl-CoA dehydrogenase (LCAD) from rat liver is highly active with both 5-cis-tetradecenoyl-CoA and 5-*trans*-tetradecenoyl-CoA. However, 5-*trans*-tetradecenoyl-CoA is a better substrate of very long-chain acyl-CoA dehydrogenase (VLCAD) than is 5-*cis*-tetradecenoyl-CoA. The overall contributions of LCAD and VLCAD to the dehydrogenation of 5-*cis*- and 5-*trans*-tetradecenoyl-CoA are still unknown.

Metabolites of hexanoyl-CoA and dodecanoyl-CoA accumulate regardless of whether palmitoyl-CoA, stearoyl-CoA, oleoyl-CoA or elaidoyl-CoA is oxidized. It may be that dodecanoyl-CoA is the intermediate that transfers from membrane-bound β-oxidation system to the matrix β-oxidation system, whereas hexanoyl-CoA may transfer from medium chain acyl-CoA dehydrogenase to short-chain acyl-CoA dehydrogenase. When Stanley and Tubbs (68) studied the metabolism of [16-C^{14}]palmitoylcarnitine, they observed an intermediate pattern with a positive correlation between abundance and chain length of intermediates. Similar results were observed when palmitoyl-CoA was used as the respiratory substrate except that hexanoyl-CoA, dodecanoyl-CoA and tetradecanoyl-CoA were found to accumulate to a greater extent. However, a relatively small amount of tetradecanoyl-CoA accumulated during the oxidation of stearoyl-CoA. It appears that the membrane-bound β-oxidation system handles palmitoyl-CoA and stearoyl-CoA differently.

Table 1: Effect of 4-Bromotiglic Acid on the Activities of β-Oxidation Enzymes in Coupled Rat Liver Mitochondria

enzyme	substrate	specific activities[a] (nmol min^{-1} mg^{-1})		remaining activity (%)
		no inhibitor	plus inhibitor	
acyl-CoA dehydrogenase	butyryl-CoA	56	53	95
	decanoyl-CoA	31	30	97
	palmitoyl-CoA	29	29	100
enoyl-CoA hydratase	crotonyl-CoA	7,000	7,300	104
	octenoyl-CoA	6,600	6,300	95
3-hydroxyacyl-CoA dehydrogenase	acetoacetyl-CoA	1,700	1,600	94
thiolase	acetoacetyl-CoA	380	33	9
	3-ketooctanoyl-CoA	500	120	24

[a]Mitochondria (1 mg/ml) were incubated with 30 μM 4-bromotiglic acid for 3 min and assayed for β-oxidation enzymes as described under Experimental Procedures.

Table II: Rates of Respiration Supported by Fatty Acid Oxidation in Coupled Rat Liver Mitochondria

Substrate	Rates of respiration[1] nmol O/min/mg of protein
9-*cis*,12-*cis*-Octadecadienoyl-CoA (Linoleoyl-CoA)	81.4 ± 1.6 (3)
9-*cis*,11-*trans*-Octadecadienoyl-CoA	64.3 ± 1.3 (3)
Decanoic acid	110.4 ± 3.3 (3)
5-*trans*,7-*trans*-Decadienoic acid	84.3 ± 1.8 (3)

[1] Values are means ± standard deviations based on the number of measurements indicated in parenthesis.

Table III: Purification of Dienoyl-CoAIsomerase and Trienoyl-CoA Isomerase from Pig Heart

Step	Total activity units		Total protein mg	Specific activity units/mg		Activity ratio DI/TI
	DI	TI		DI	TI	
Soluble extract	760	22	11340	0.067	0.002	34.5
PEG precipitation	774	20	2780	0.278	0.007	38.7
Q-Sepharose	590	11	207	2.85	0.053	53.6
Hydroxyapatite	363	6.8	86	4.22	0.079	53.4
Chromatofocusing	174	2.1	15.6	11.1	0.134	82.8
Sepharose CL-6B/ Reactive Red 120	56	0.39	0.58	96	0.67	143

[1] DI, dienoyl-CoA isomerase; TI, trienoyl-CoA isomerase.

Table IV: Contents of FAD, FMN, Iron and Labile Sulfur in 2,4-Dienoyl-CoA Reductase from *E. coli*

cofactor	enzyme calculated	cofactor determined	ratio (cofactor/enzyme)
FAD	0.96 nmol	0.82±5e-3(3) nmol[a]	0.85
	38.4 nM	37.8±0.6(3) nM[b]	0.98
FMN	0.96 nmol	0.82±9e-3(3) nmol[a]	0.85
	38.4 nM	37.7±0.2(3) nM[b]	0.98
Fe	3.20 nmol	12.32 nmol	3.9
Sulfur	1.50 nmol	6.50 nmol	4.3

a: FAD or FMN content determined by HPLC;
b: FAD or FMN content determined by fluorescence spectrophotometry.

Table V: Recovery of Enzyme Activity and Iron after Anaerobic Titration

	total activity (mU)	Fe content (nmol)
before anaerobic titration	252	12.32
after anaerobic titration	259	
concentrated enzyme	242	11.8
filtrate	< 1	< 0.1

E. coli reductase was first titrated with either NADPH or dithionite anaerobically and then the mixture was subsequently exposed to air. The mixture was concentrated with an Amicon concentrator. Enzyme activity and Fe content were determined for both the concentrated enzyme and the filtrate.

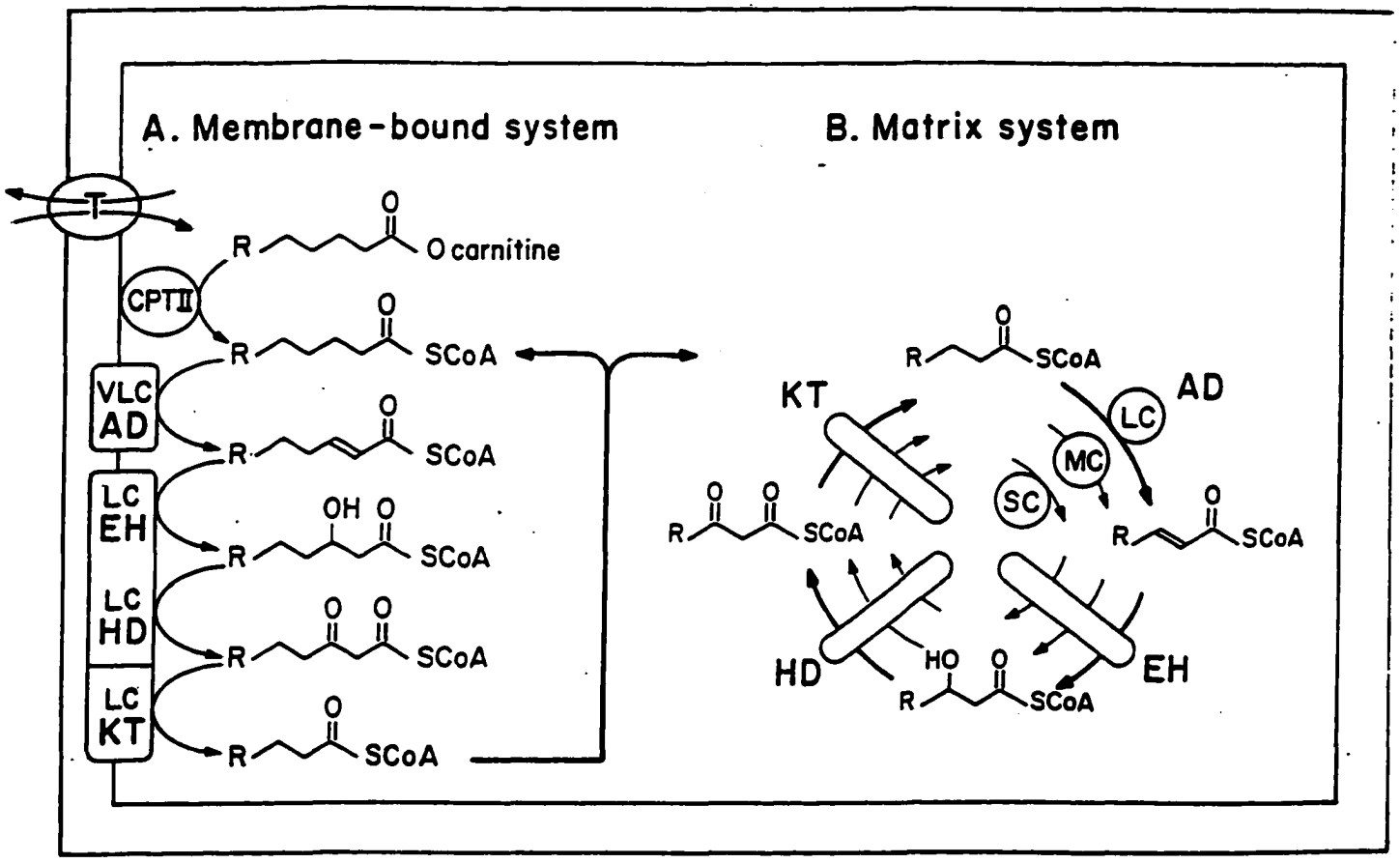

Figure 1. Model of the functional and physical organization of β-oxidation enzymes in mitochondria.

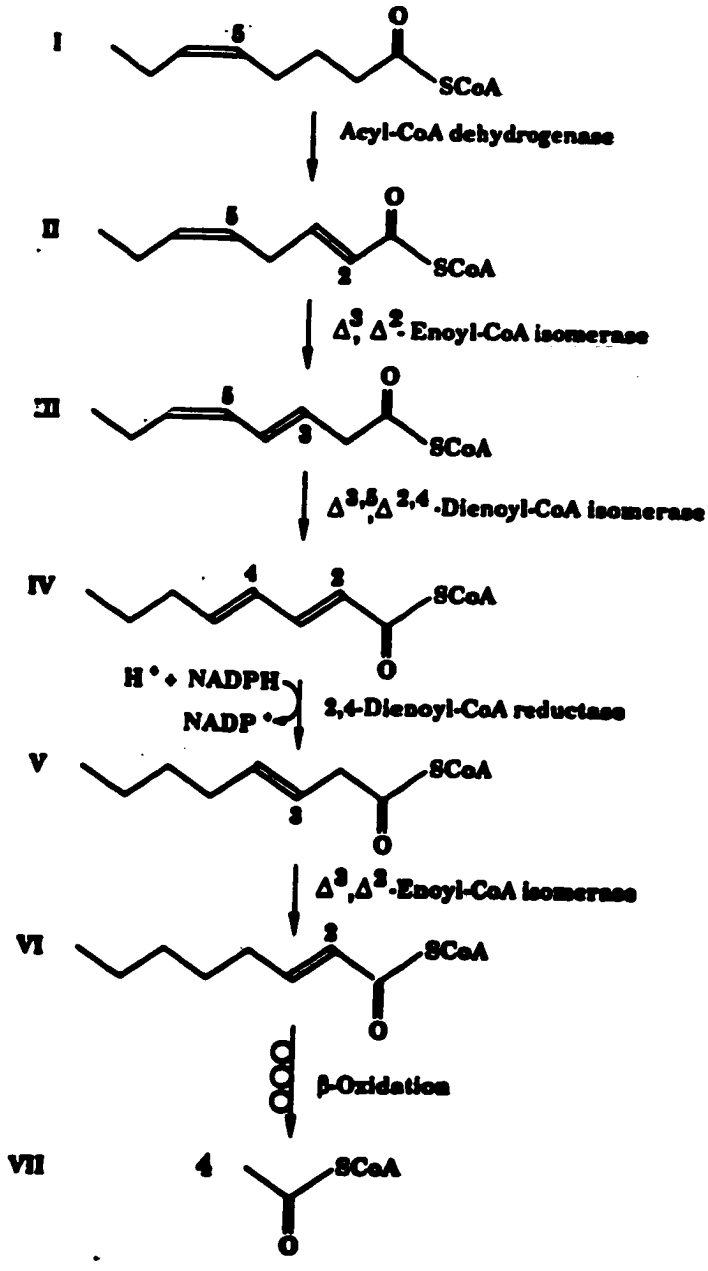

Figure 2. Proposed pathway of the NADPH-dependent β-oxidation of 5-*cis*-octanoyl-CoA.

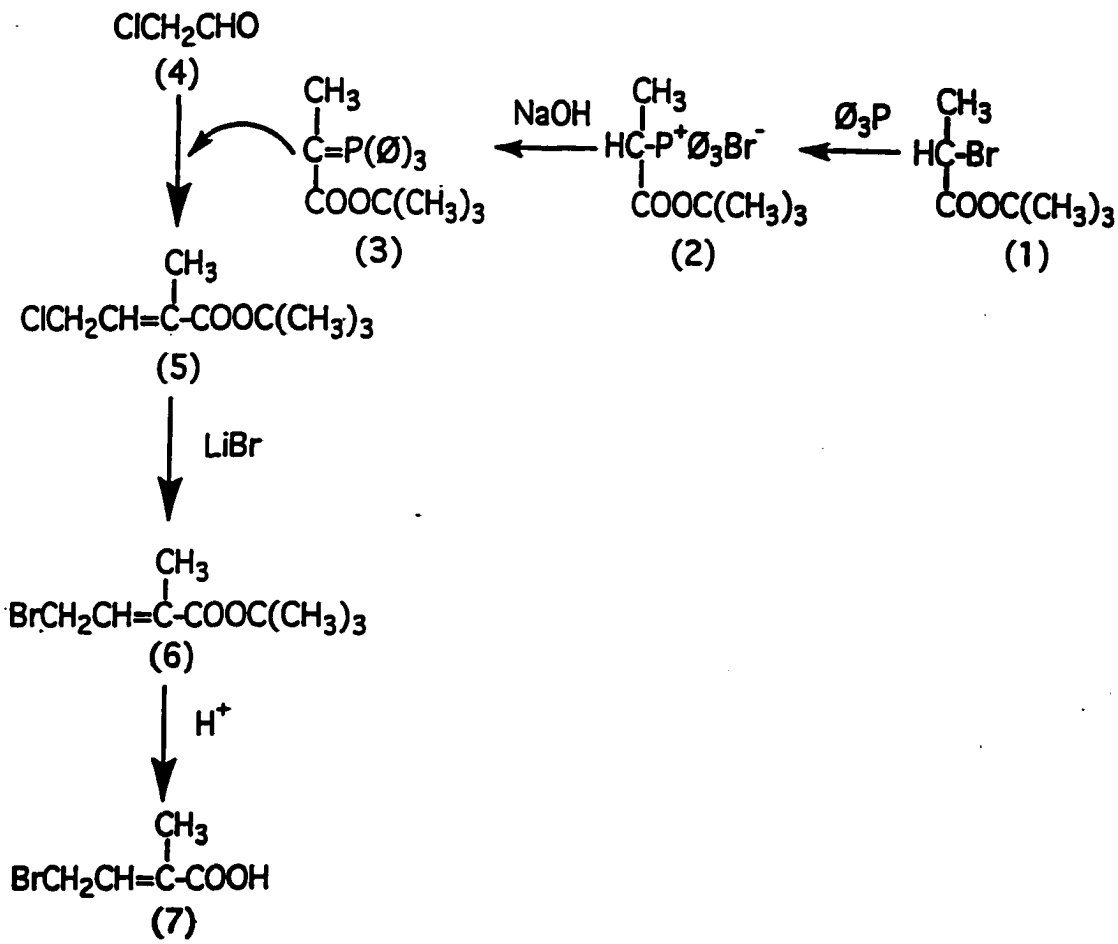

Figure 3. Synthesis of 4-bromotiglic acid.

A. No inhibitor

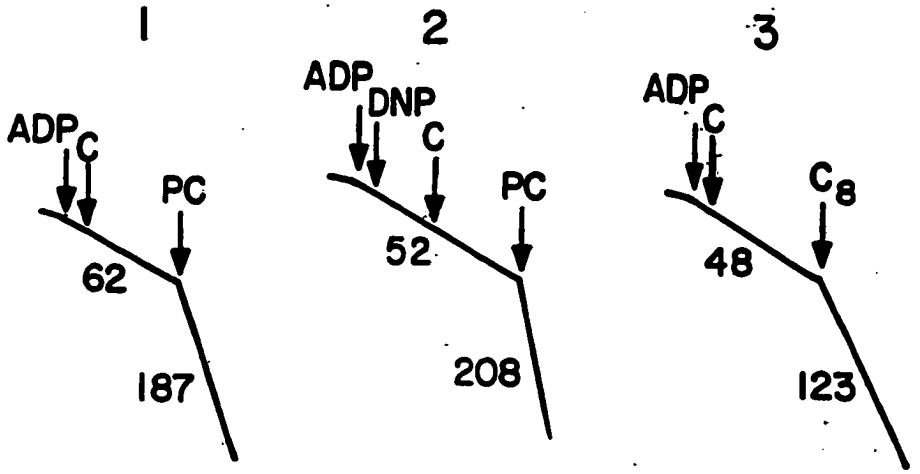

B. With inhibitor

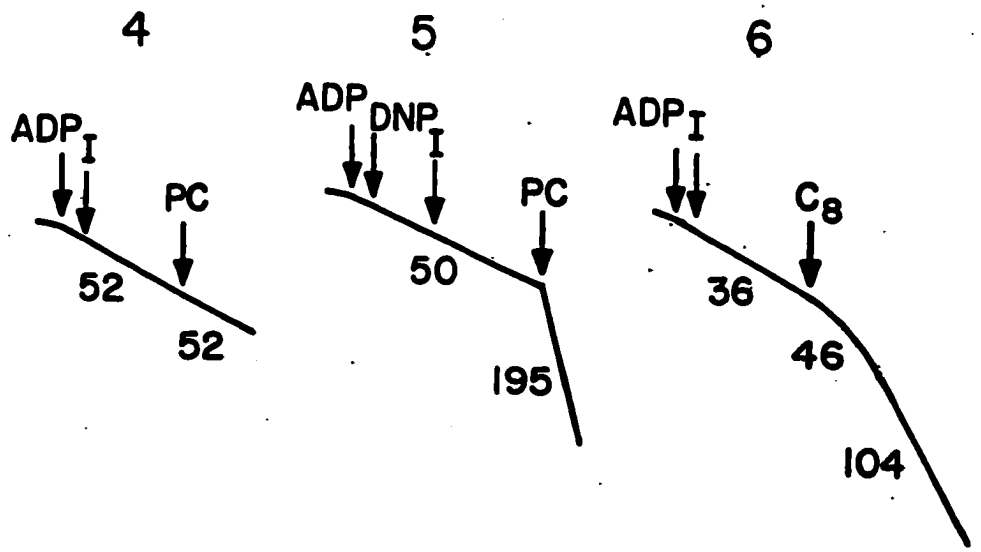

Figure 4. Effect of 4-bromotiglic acid on mitochondrial respiration supported by either palmitoylcarnitine or octanoate. For experimental details see Experimental Procedure: PC, 15 μM palmitoylcarnitine; C_8, 0.1 mM octanoate; I, 10 μM 4-bromotiglic acid in 1M Tris-HCl (pH 7.2) containing 1 M KCl; C, carrier of inhibitor; and DNP, 0.1 mM 2,4-dinitrophenol. The numbers represent the rates of respiration in nanoatoms of O_2/min/mg of protein.

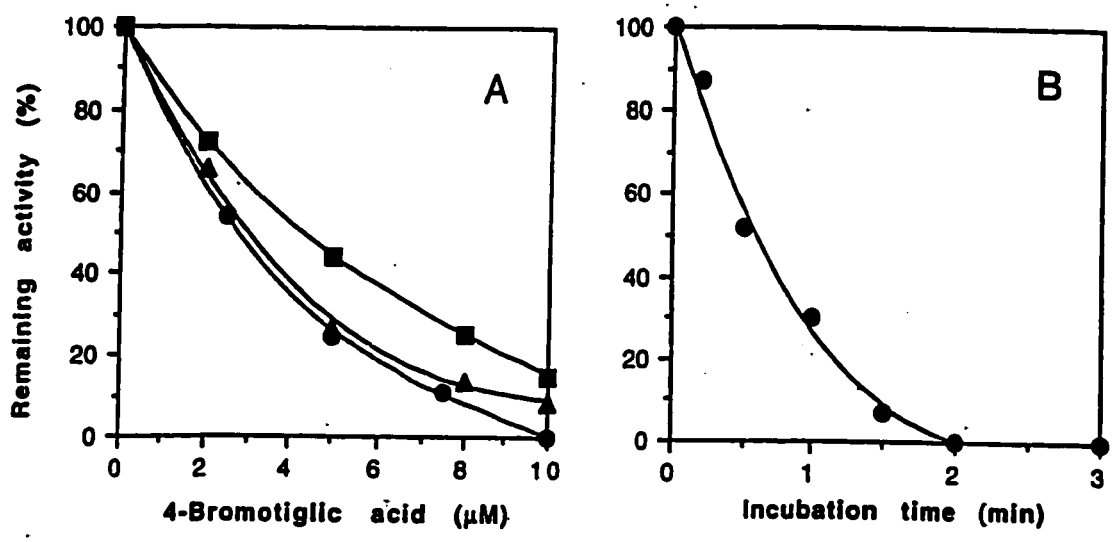

Figure 5. Inhibitions of respiration and thiolase activities in coupled rat liver mitochondria as functions of the 4-bromotiglic acid concentration (A) and the incubation time (B): A, The incubation was 2 min; B, the concentration of 4-bromotiglic acid was 10 μM; (●) respiration supported by palmitoylcarnitine; (▲) thiolase assayed with acetoacetyl-CoA; (■) thiolase assayed with 3-ketooctanoyl-CoA. Thiolase activities are based on three measurements with standard deviations of 6% or less of the mean values.

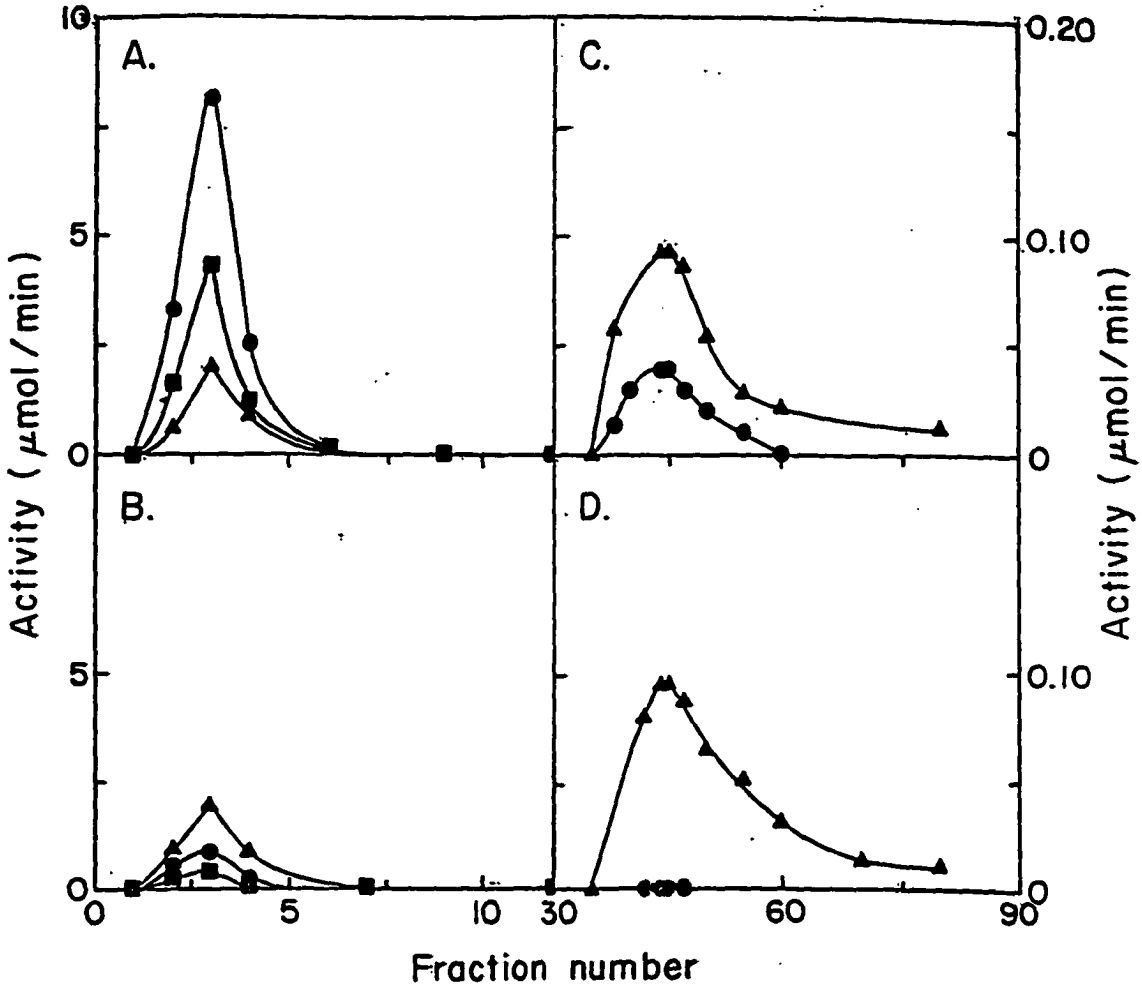

Figure 6. Separation of thiolases present in a homogenate of rat liver mitochondria by chromatography on DEAE-cellulose. (A, B) Flow-through fractions containing soluble 3-ketoacyl-CoA thiolase, acetoacetyl-CoA thiolase, and 3-hydroxyacyl-CoA dehydrogenase. (C, D) Fractions eluted with a KCl gradient contained long-chain 3-ketoacyl-CoA thiolase and long-chain 3-hydroxyacyl-CoA dehydrogenase. (A, C) Homogenate from control mitochondria. (B, D) Homogenate from mitochondria preincubated with 4-bromotiglic acid. For experimental details see under Experimental Procedures: thiolase activities detected with acetoacetyl-CoA (■) and with 3-ketooctanoyl-CoA (●); 3-hydroxyacyl-CoA dehydrogenase measured with 3-ketooctanoyl-CoA as substrate (▲).

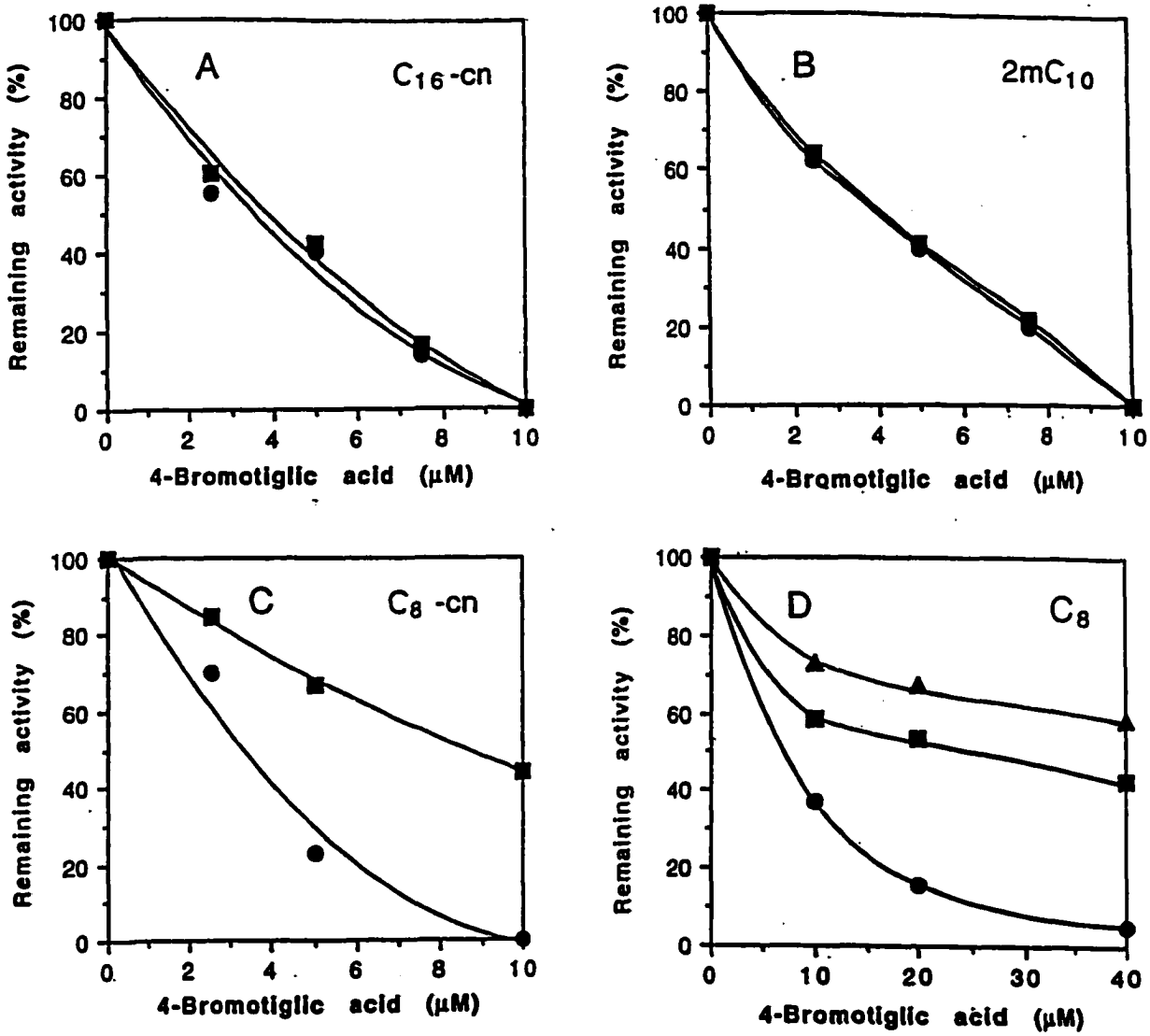

Figure 7. Inhibition of respiration supported by various substrates of β-oxidation as a function of the concentration of 4-bromotiglic acid. Coupled rat liver mitochondria (0.5 mg/ml) were preincubated for 2 min with the indicated concentrations of 4-bromotiglic acid. Substrates were added and rates of respiration were measured in the presence of the inhibitor (●) or after removing the inhibitor (■) by centrifuging the mitochondrial suspension for 30 s at 13,000 x g and resuspending the pellet in the same incubation buffer except that 4-bromotiglic acid was omitted. Substrates were A, palmitoylcarnitine (C_{16}-cn); B, 2-methyldecanoic acid ($2mC_{10}$); C, octanoylcarnitine (C_8-cn); and D, octanoic acid (C_8). (D) Relative rates of respiration: (●) initial rates in the presence of the inhibitor; (▲) steady-state rates in the presence of the inhibitor; and (■) rates after removal of the inhibitor. The relative rates are based on the means of three measurements with standard deviations of 10% or less of the mean values.

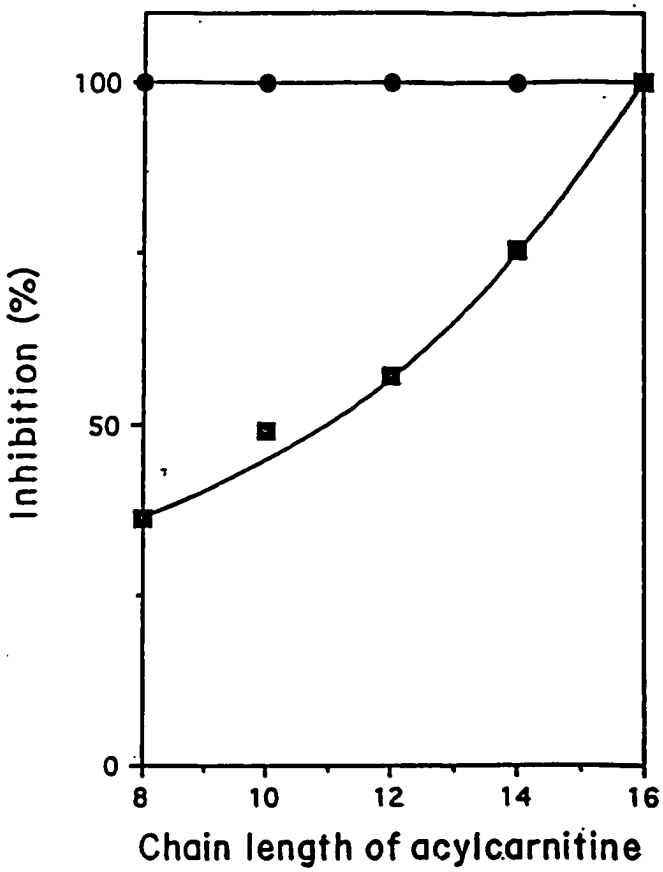

Figure 8. Inhibition of respiration as a function of the acylcarnitine chain length. Acylcarnitines with acyl chains having 8-16 carbon atoms served as substrates. Inhibition observed in the presence (●) and absence (■) of inhibitor after preincubating mitochondria (0.5 mg/ml) with 10 μM 4-bromotiglic acid for 2 min. Values of inhibition are based on the means of three measurements with standard deviations of 6% or less of the mean values.

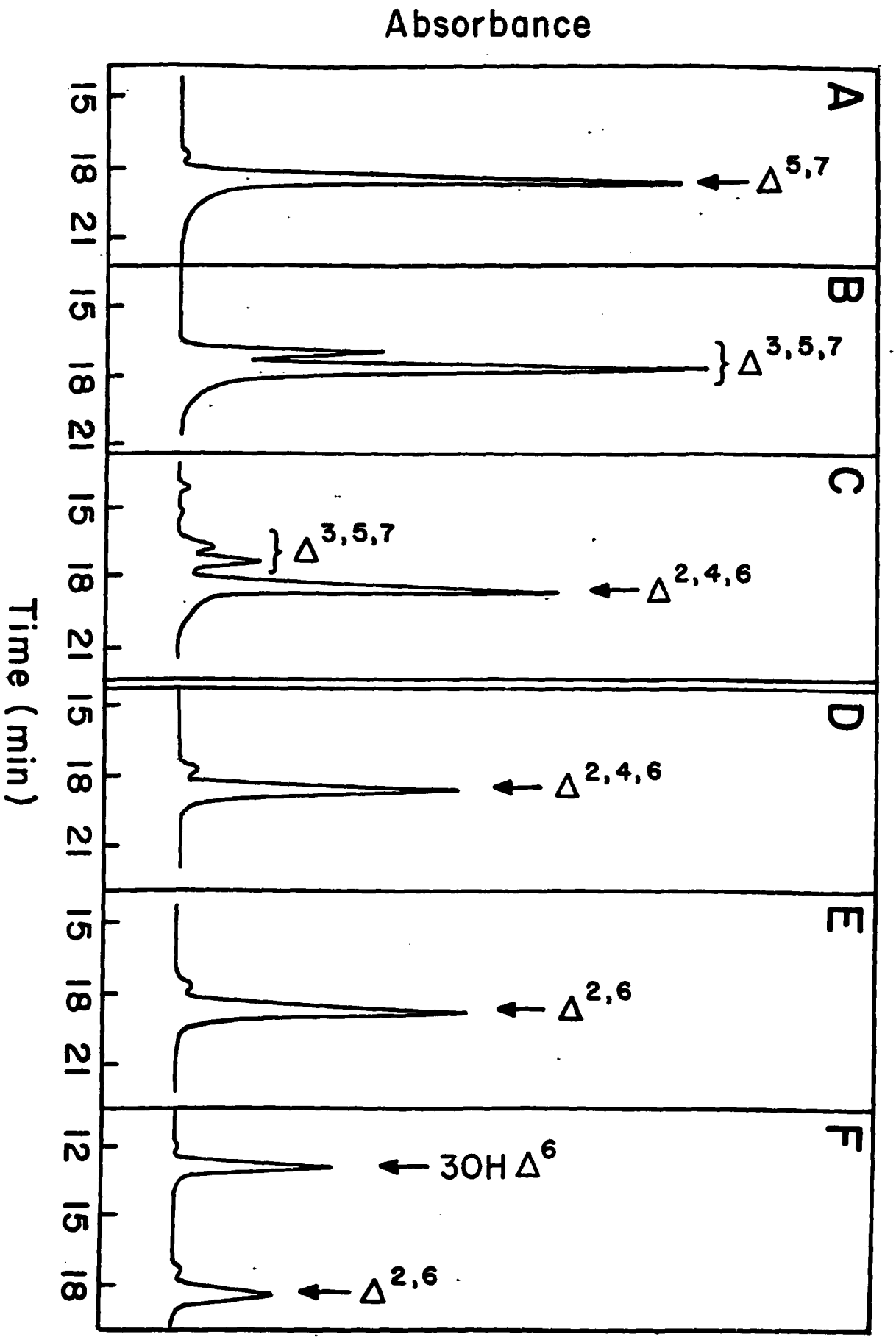

Figure 9. HPLC analysis of metabolites formed by enzymatic conversions of 5,7-decadienoyl-CoA. A. HPLC-purified 5,7-decadienoyl-CoA ($\Delta^{5,7}$). B. 3,5,7-Decatrienoyl-CoA ($\Delta^{3,5,7}$) formed from 5,7-decadienoyl-CoA (8 nmol in 0.2 ml of 0.1 M KPi, pH 8.0) by acyl-CoA oxidase (0.1 unit) and peroxisomal multifunctional protein I (6 μg) within 10 min. C. 2,4,6-Decatrienoyl-CoA ($\Delta^{2,4,6}$) formed from 3,5,7-decatrienoyl-CoA, described under B, by dienoyl-CoA isomerase (0.4 unit). D. HPLC-purified 2,4,6-decatrienoyl-CoA after incubation without or with crotonase (0.7 unit). E. 2,6-Decadienoyl-CoA ($\Delta^{2,6}$) formed from HPCL-purified 2,4,6-decatrienoyl-CoA (10 nmol in 0.5 ml of 0.1 M KPi, pH 8.0) by *E. coli* 2,4-dienoyl-CoA reductase (5 μg) plus 0.1 mM NADPH within 5 min. F. 3-Hydroxydece-6-noyl-CoA (3OHΔ^{6}) formed from half of the sample described under E by crotonase (0.7 unit) within 1 min.

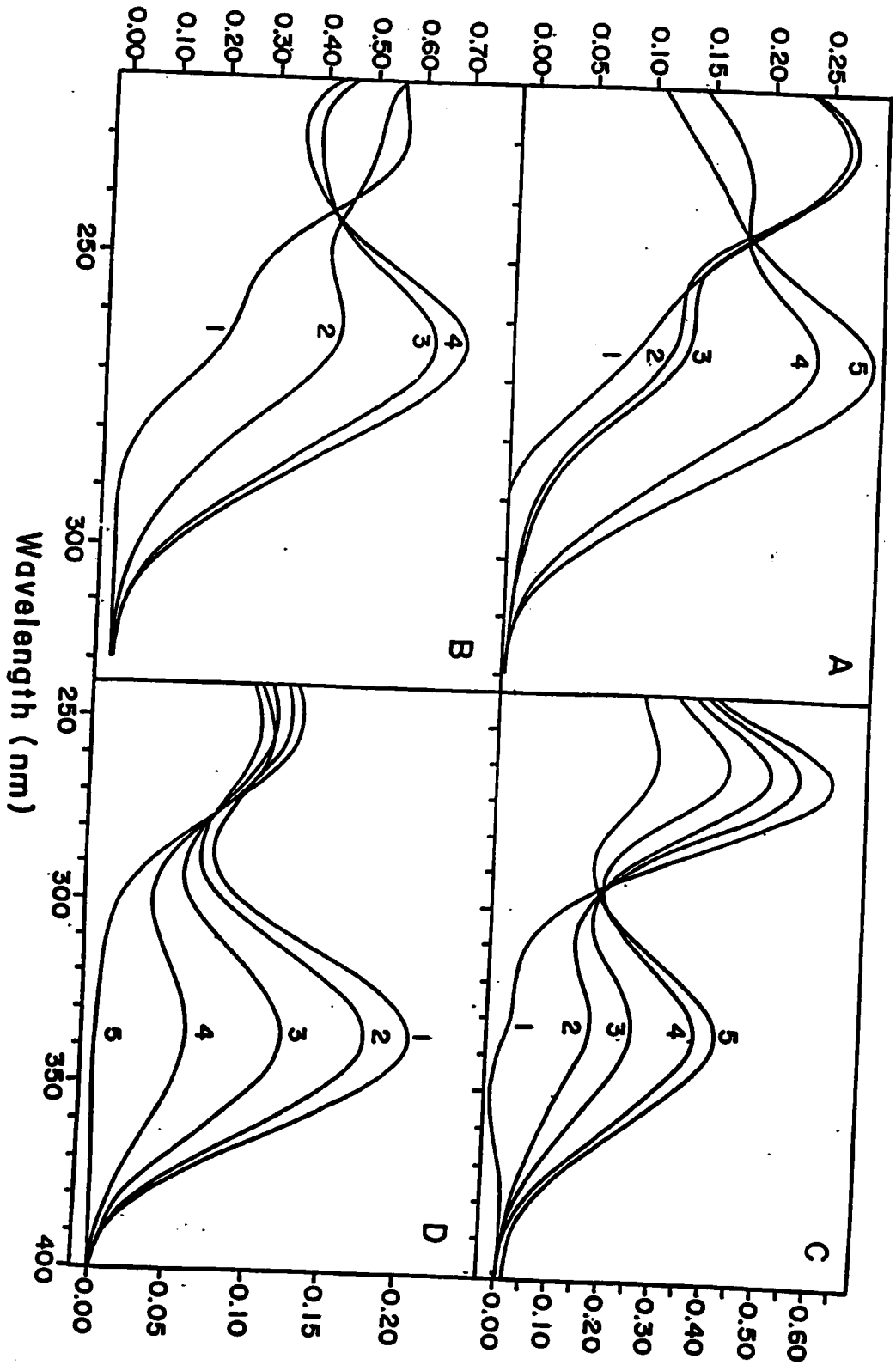

Figure 10. Spectrophotometric analysis of enzymatic conversions of 5,7-decadienoyl-CoA and its metabolites. A. Spectral changes associated with the dehydrogenation of 5,7-decadienoyl-CoA (7 μM in 0.1 M KPi, pH 9) by acyl-CoA oxidase (30 milliunits/ml) and isomerization of 2,5,7-decatrienoyl-CoA to 3,5,7-decatrienoyl-CoA by enoyl-CoA isomerase (0.15 μg/ml). Spectrum 1, 5,7-decadienoyl-CoA at time zero; Spectrum 2, 30 s after the addition of acyl-CoA oxidase (ACO); Spectrum 3, 3 min or 30 min after the addition of ACO; Spectrum 4, 30 s after the addition of enoyl-CoA isomerase (ECI) to the sample with spectrum 3; Spectrum 5, 2 min after the addition of ECI. B. Spectral changes associated with the conversion of 5,7-decadienoyl-CoA to 3,5,7-decatrienoyl-CoA catalyzed by acyl-CoA oxidase and enoyl-CoA isomerase. Spectrum 1, 5,7-decadienoyl-CoA (19 μM in 0.1 M KPi, pH 8.0). Spectrum 2, 15 s after the addition of acyl-CoA oxidase (0.15 unit/ml) and peroxisomal multifunctional protein I (10 μg/ml); Spectrum 3, 1 min after enzyme addition; Spectrum 4, 3 min after enzyme addition. C. Spectral changes associated with the isomerization of 3,5,7-decatrienoyl-CoA to 2,4,6-decatrienoyl-CoA catalyzed by a soluble extract of rat liver mitochondria or partially purified dienoyl-CoA isomerase. Spectrum 1, 3,5,7-Decatrienoyl-CoA (20 μM in 0.1 M KPi, pH 8.0). Spectra 2-4, 3 min, 7 min, and 30 min after the addition of enzyme; Spectrum 5, HPLC-purified 2,4,6-decatrienoyl-CoA. D. Spectral changes associated with the reduction of 2,4,6-decatrienoyl-CoA by NADPH in the presence of purified 2,4-dienoyl-CoA reductase from *E. coli*. Spectrum 1, 2,4,6-decatrienoyl-CoA (4 μM in 0.1 M KPi, pH 8.0), NADPH (0.1 mM) was added to the sample and reference and the reaction was initiated by the addition of 2,4-dienoyl-CoA reductase (0.5 μg). Spectra 2-5, 15 sec, 1 min, 2.5 min, and 6 min after starting the reaction.

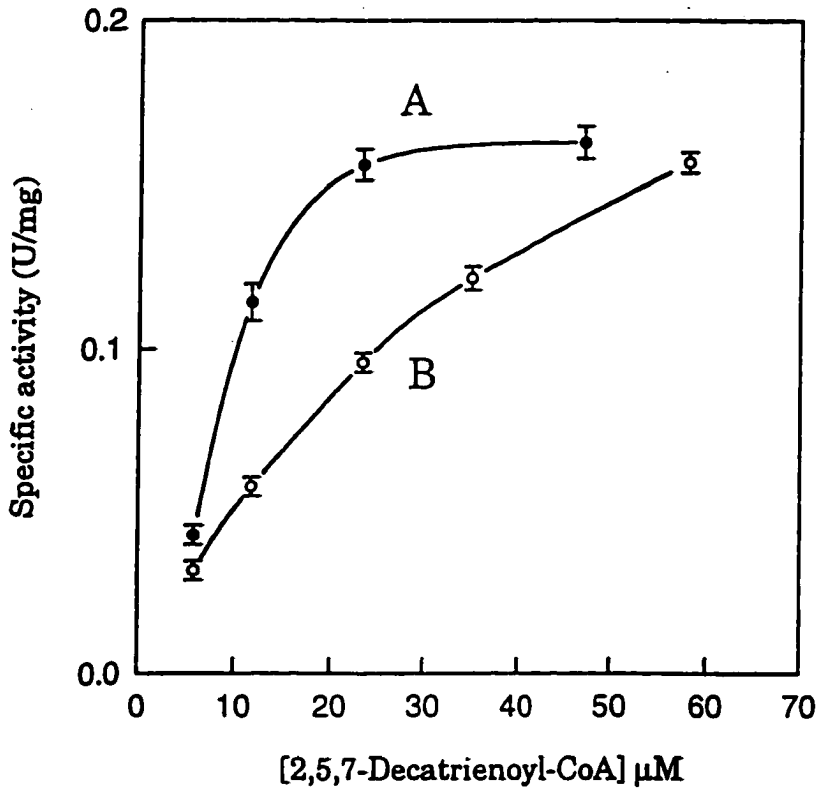

Figure 11. Rates of 2,5,7-decatrienoyl-CoA metabolism by a soluble extract of rat liver mitochondria as a function of the substrate concentration. A, rate of NADH formation in the presence of 1 mM NAD^+ and 0.3 mM CoASH. B, rates of 2,4,6-decatrienoyl-CoA formation in the presence of trienoyl-CoA isomerase (0.25 unit/ml) but in the absence of coenzymes.

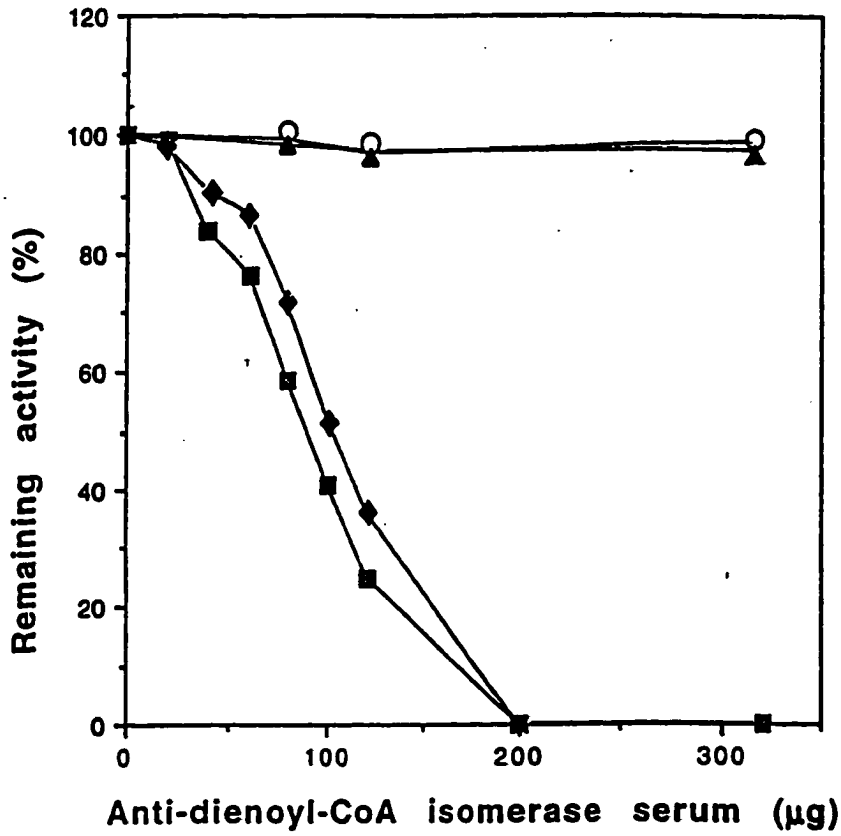

Figure 12. Immunoprecipitation of dienoyl-CoA isomerase and trienoyl-CoA isomerase activities present in a partially purified preparation of dienoyl-CoA isomerase by serum raised against purified dienoyl-CoA isomerase from rat liver. For details see under Experimental Procedures. Activities of dienoyl-CoA isomerase (○,■) and trienoyl-CoA isomerase (▲,◆) remaining in the supernatant. Antiserum (■,◆), preimmune serum(○,▲).

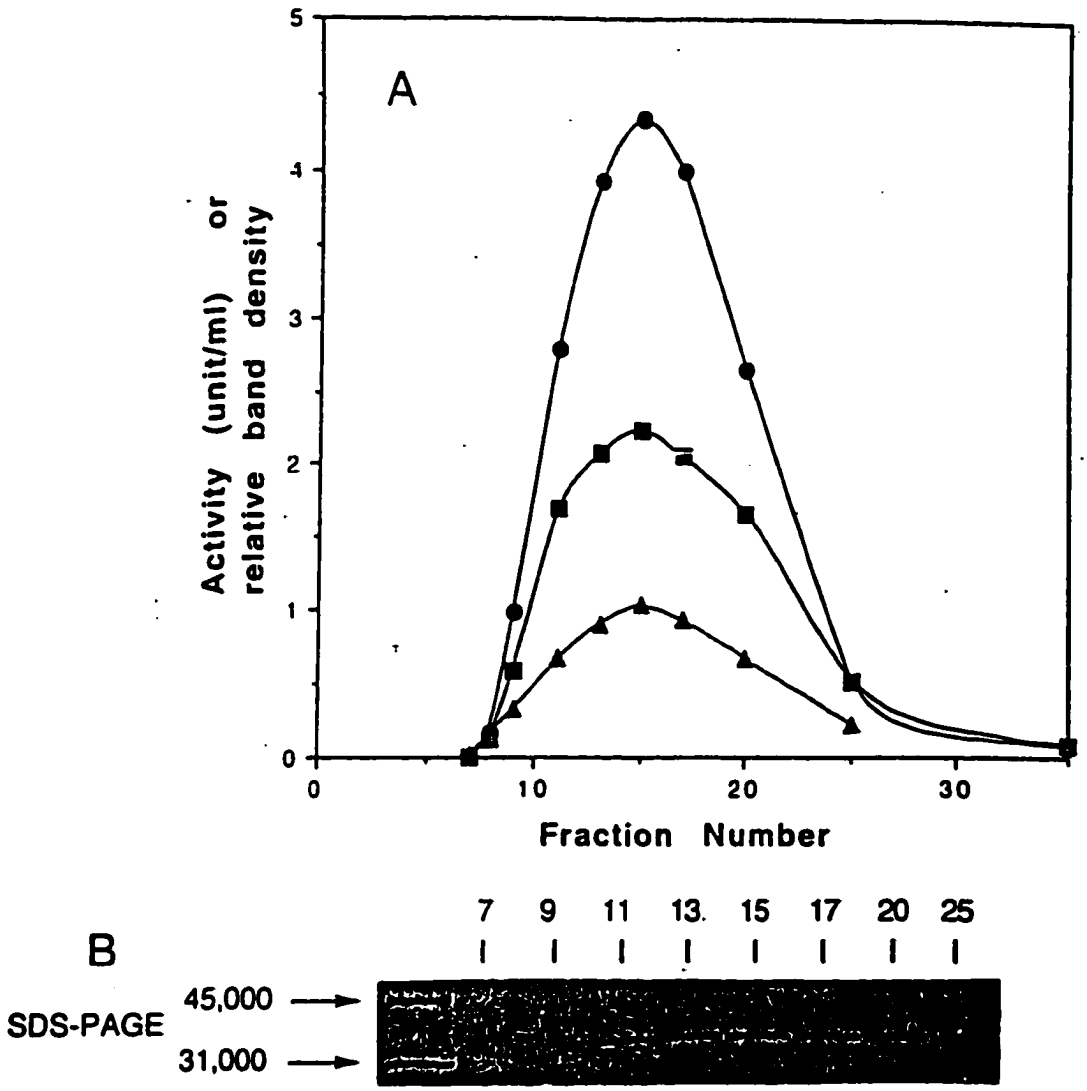

Figure 13. Analysis of fractions eluted from a Reactive Red 120 column during the final purification step of trienoyl-CoA isomerase. A, fractions were assayed for trienoyl-CoA isomerase (■) (values were multiplied by 75), dienoyl-CoA isomerase (●), and protein (▲) based on the relative densities of bands shown in panel B. B. Fractions were subjected to SDS-PAGE and stained for protein with Coomassie brilliant blue.

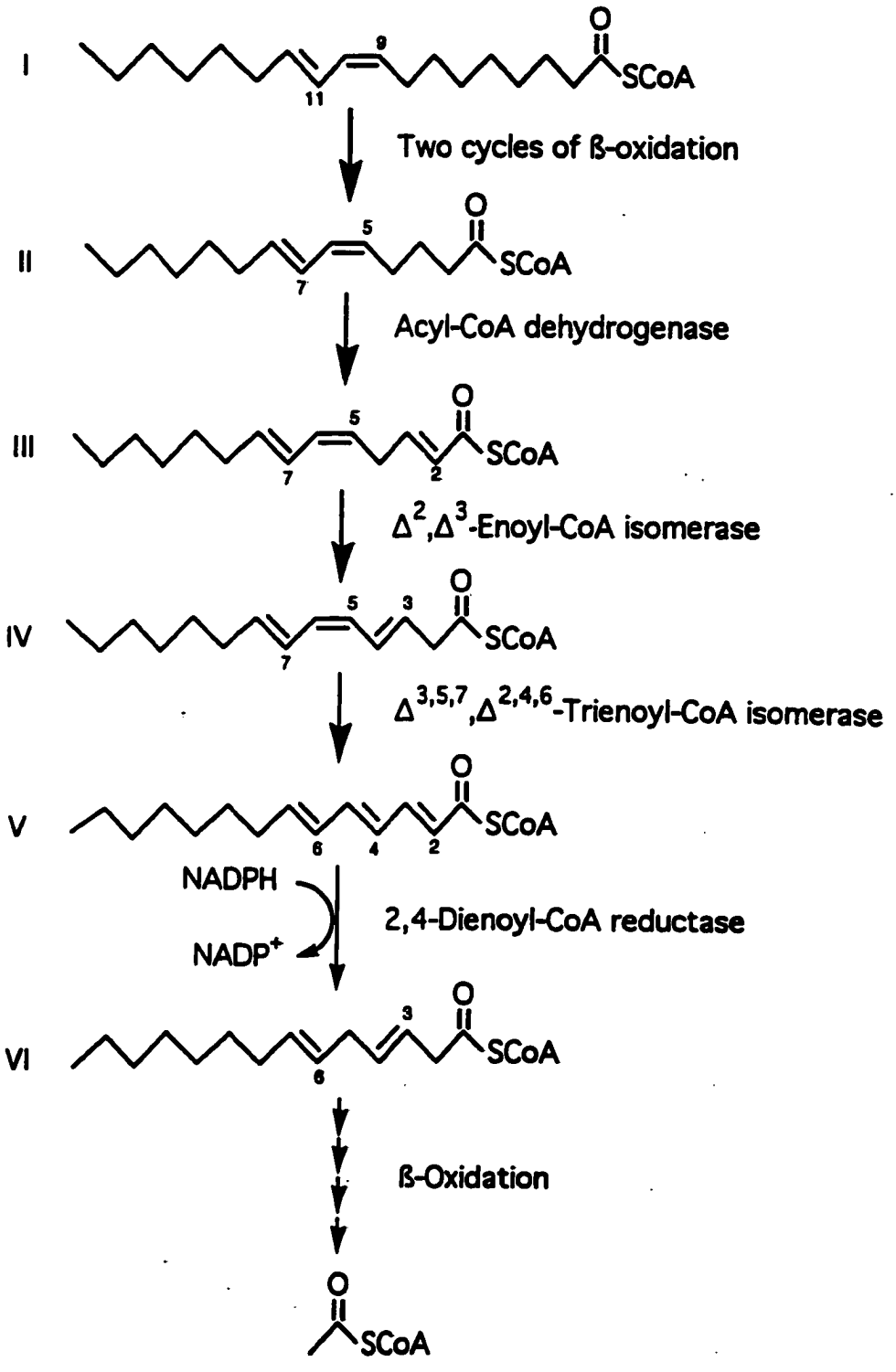

Figure 14. Proposed trienoyl-CoA isomerase-dependent pathway for the β-oxidation of 9-*cis*,11-*trans*-octadecadienoyl-CoA (conjugated linoleoyl-CoA).

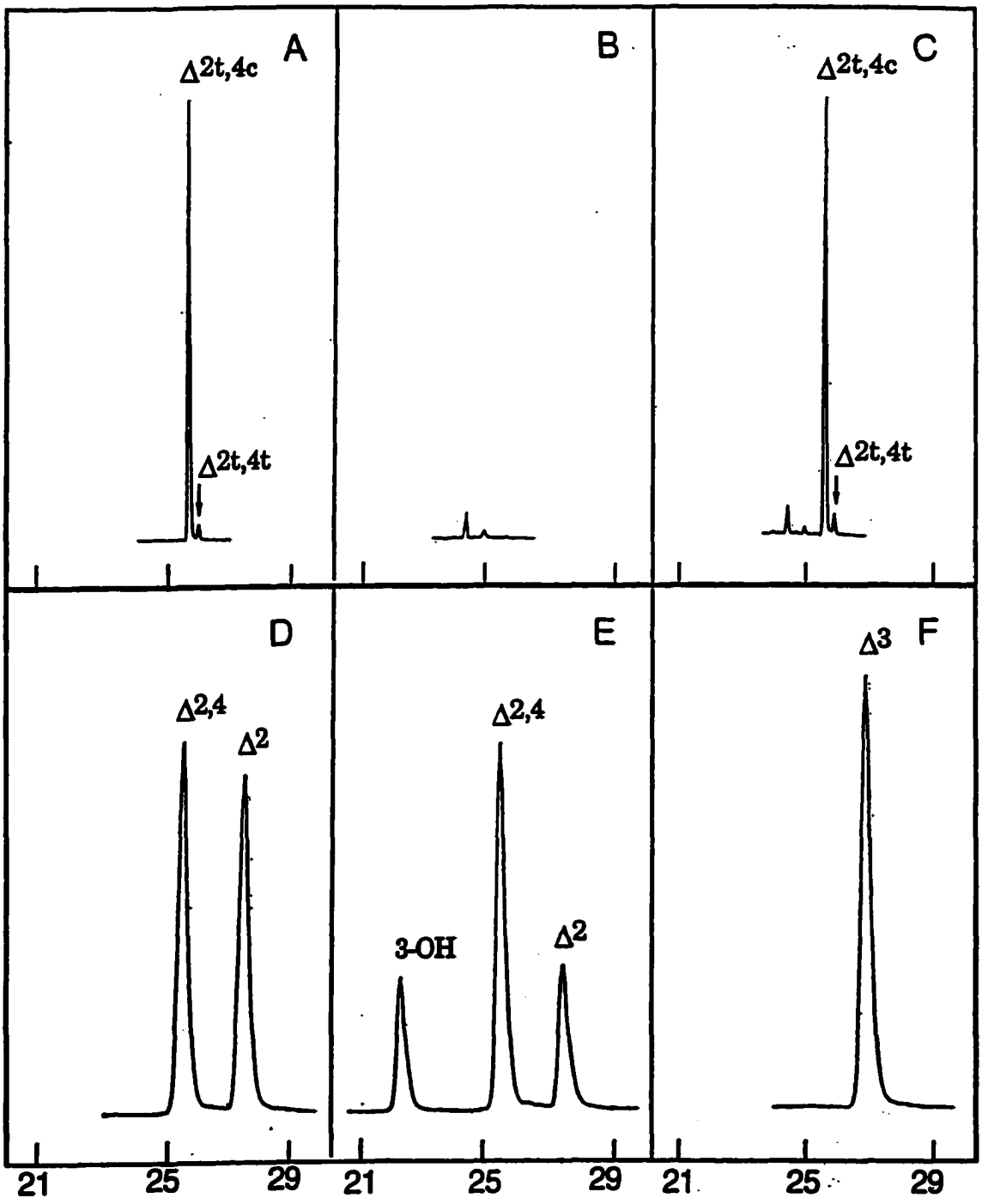

Figure 15. Evaluation of 2,4-dienoyl-CoA reductase from *E. coli* for *cis* → *trans* isomerase activity and Δ^3,Δ^2-enoyl-CoA isomerase activity. Panel A, 2.2 nmol of HPLC-purified 2-*trans*,4-*cis*-decadienoyl-CoA. Panel B, 0.6 nmol of purified 2,4-dienoyl-CoA reductase. Panel C, 2.2 nmol of 2-trans,4-cis-decadienoyl-CoA after incubation for 30 sec with 0.6 nmol of reductase in 270 ul of 50 mM KPi (pH 7.4) in the absence of NADPH. Panel D, 4.5 nmol of 2-*trans*,4-*cis*-decadienoyl-CoA after incubation for 3 min with 0.15 μg of 2,4-dienoyl-CoA reductase in 270 ul of 50 mM KPi (pH 7.4) in the presence of 0.1 mM NADPH. Panel E, the same as D but in the presence of 0.42 mU of crotonase. Panel F, 2.8 nmol of 3-*trans*-decenoyl-CoA after incubation with 0.15 μg of reductase in the presence of 0.42 mU of crotonase.

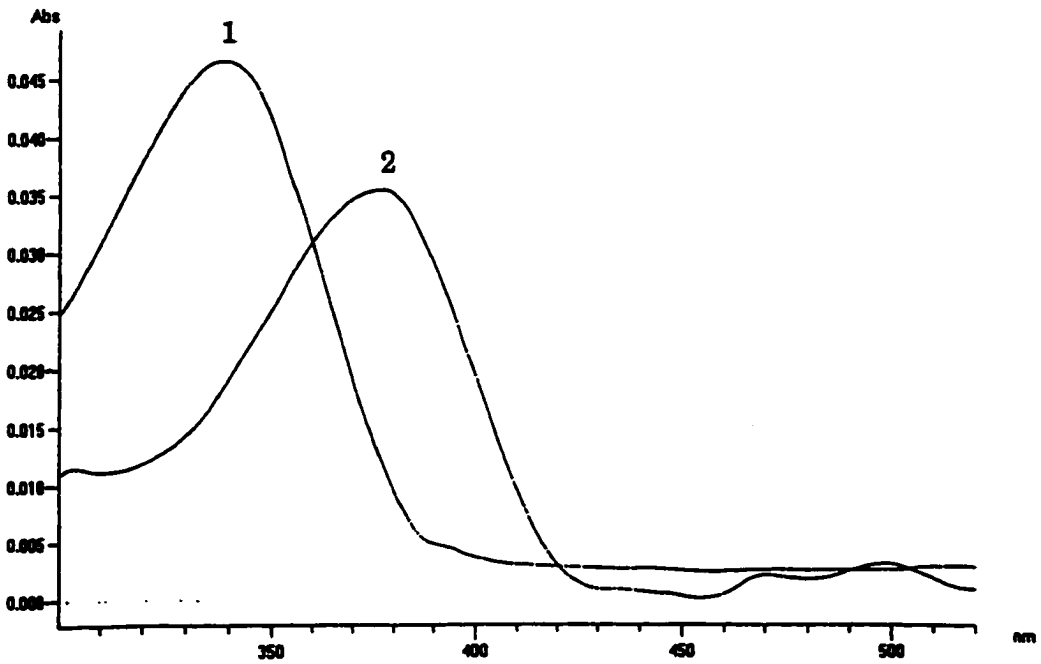

Figure 16. Spectral shift of 5-phenyl-2,4-pentadienoyl-CoA induced by binding to *E.coli* 2,4-dienoyl-CoA reductase. Spectrum 1, 0.74 μM 5-phenyl-2,4-pentadienoyl-CoA in 60 mM KPi (pH 7.4) containing 1 mM EDTA and 5 mM mercaptoethanol. Spectrum 2, 0.74 μM 5-phenyl-2,4-pentadienoyl-CoA bound to 20.8 μM *E. coli* 2,4-dienoyl-CoA reductase under the conditions specified for Spectrum 1. Spectrum 2 was corrected for the absorbance of the enzyme.

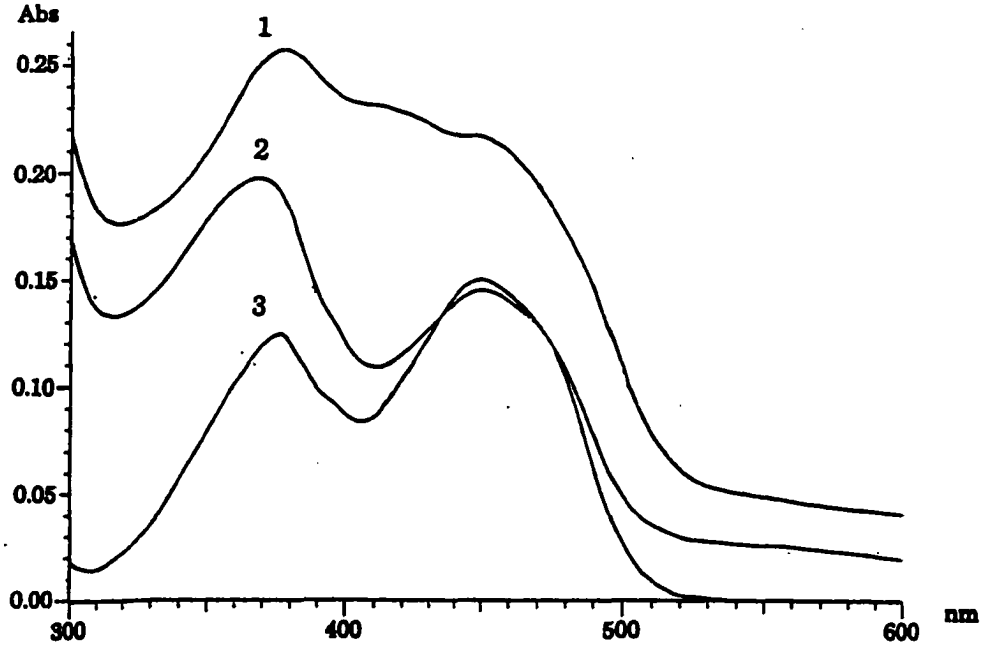

Figure 17. Spectral changes of *E. coli* 2,4-dienoyl-CoA reductase in the presence of 8 M guanidine hydrochloride (GuHCl). 1: spectrum of the native enzyme (6.25 μM) in 0.1 M potassium phosphate (pH 7.7) containing 0.1 mM EDTA; 2: spectrum of the denatured enzyme (6.25 μM) in the presence of 8 M GuHCl; 3: spectrum of an equimolar mixture (6.25 μM each) of free FAD and FMN in the GuHCl.

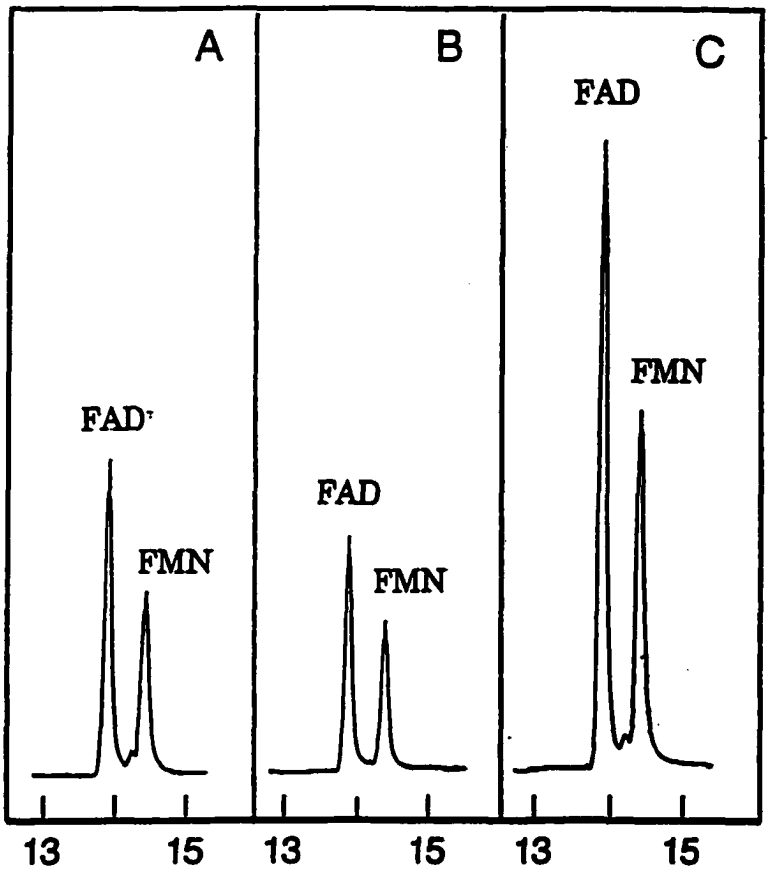

Figure 18. Evidence for the presence of an equimolar amount of FAD and FMN in 2,4-dienoyl-CoA reductase from *E. coli*. Panel A, a mixture of 0.492 nmol of free FAD and 0.486 nmol of free FMN. Panel B, FAD and suspected FMN released from 0.48 nmol of purified *E. coli* reductase. Panel C, a mixture of the samples shown in panels A and B.

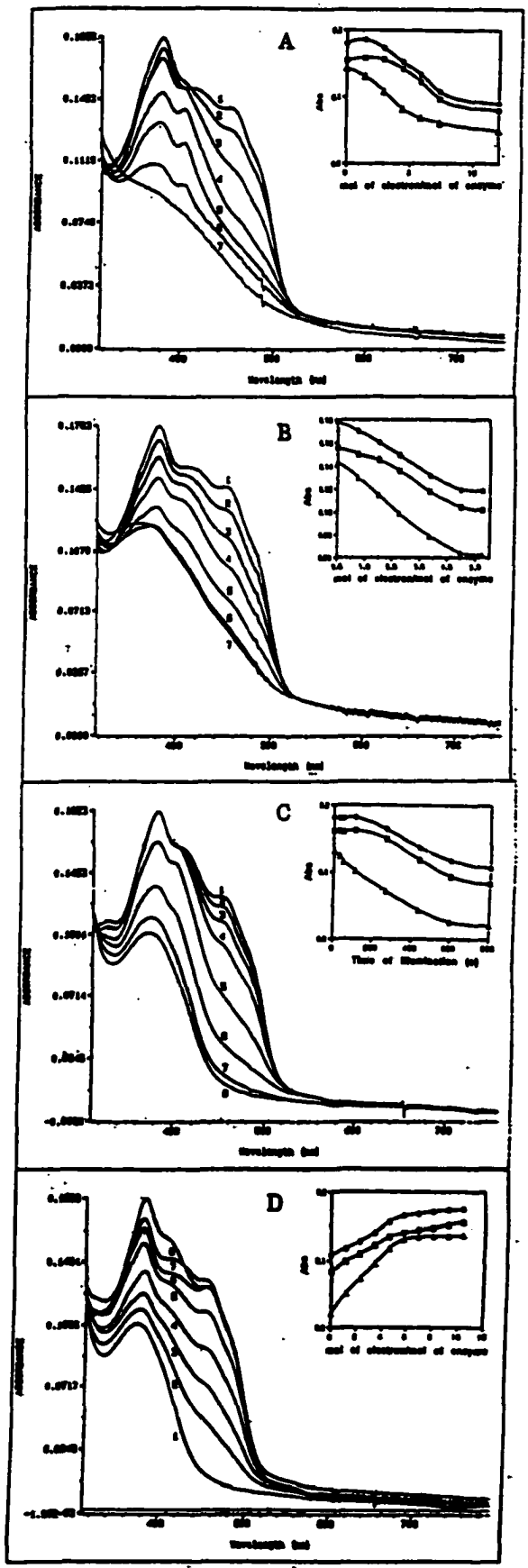

Figure 19. Anaerobic titration and photoreduction of 2,4-dienoyl-CoA reductase from *E. coli*.

Panel A. Dithionite reduction of *E. coli* reductase. An anaerobic solution of enzyme (4.2 μM enzyme in 0.8 ml of 60 mM potassium phosphate buffer, pH 7.4, 25°C) was titrated with a solution of 2.48 mM dithionite. Spectrum 1, at 0 min, no addition; 2, 1.48 mol at 2 min; 3, 2.95 mol at 8 min; 4, 4.43 mol at 16 min; 5, 5.90 mol at 59 min; 6, 7.38 mol at 3 hr; 7, 12.0 mol at 8 hr of electron/mol enzyme. Intermediate spectra have been omitted for clarity.

Panel B. NADPH reduction of *E. coli* 2,4-dienoyl-CoA reductase. An anaerobic solution of enzyme (4.2 μM enzyme in 0.8 ml of 60 mM potassium phosphate buffer, pH 7.4, 25°C) was titrated with 0.63 mM NADPH. Curve 1, 0 mol at 0 min; 2, 0.75 mol at 2 min; 2, 1.50 mol at 5 min; 3, 2.25 mol at 6 min; 4, 3.38 mol at 7 min 30 s; 5, 4.50 mol at 9 min 30 s; 6, 5.25 mol at 11 min of electron/mol enzyme. Intermediate spectra have been omitted for clarity.

Panel C. Effect of deazaflavin on the photoreduction of *E. coli* 2,4-dienoyl-CoA reductase. An anaerobic solution of enzyme (3.9 μM enzyme in 0.8 ml of 60 mM potassium phosphate buffer, pH 7.4, 0°C, containing 2 mM EDTA and 1 μM deazaflavin) was illuminated in the dark with a 150-W flush light. Spectra were recorded after each illumination periods. (Spectra 1-8) after 0, 30 s, 50 s, 110 s, 270 s, 440 s, 600 s, 800 s of illumination. Only selected spectra are shown.

Panel D. Back titration of fully reduced *E. coli* 2,4-dienoyl-CoA reductase with ferricynanide. Oxidized reductase (3.9 μM enzyme in 0.8 ml of 60 mM potassium phosphate buffer, pH 7.4, 0°C, containing 2 mM EDTA and 1 μM deazaflavin) was fully

reduced anaerobically by irradiation and then back-titrated with an anaerobic solution of 3.6 mM ferricyanide. Spectrum 1, fully reduced enzyme at 0 min; 1.15 mol at 20 s; 2, 2.30 mol at 1 min; 3, 3.45 mol at 1 min 50 s; 4, 4.6 mol at 2 min 30 sec; 5, 5.75 mol at 3 min; 6, 8.05 mol at 4 min 25 s; 7, 9.20 mol at 8 min of ferricynanide/mol enzyme. Only selected spectra are shown.

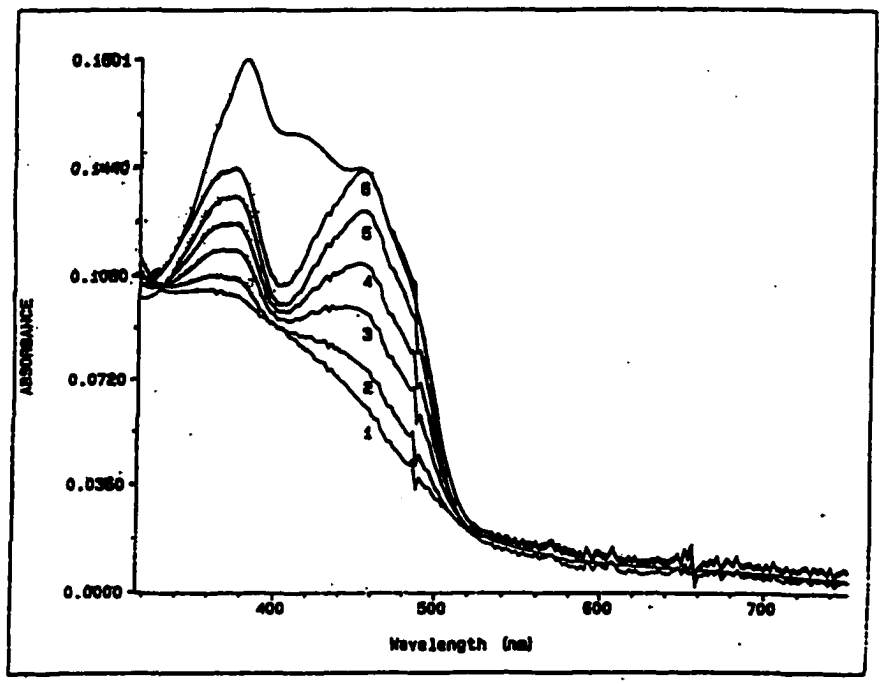

Figure 20. Reoxidation of reduced *E. coli* reductase under aerobic condition. *E. coli* reductase (4.2 μM enzyme) was reduced under anaerobic condition with dithionite. The anaerobic solution was then exposed to air to allow the reduced enzyme to be reoxidized. Spectrum 1, reduced enzyme at 0 min; Spectrum 2 to 6, 6, 8, 10, 14, 41 min after exposing the solution to air, respectively; Spectrum 7, native enzyme.

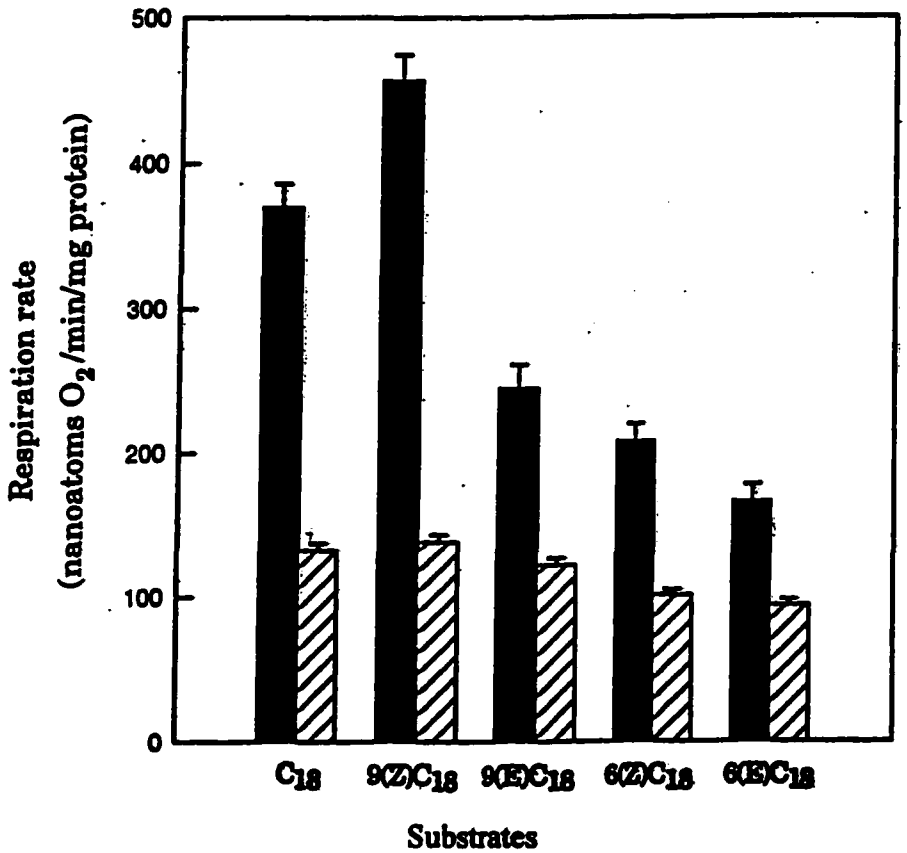

Figure 21. Rates of respiration supported by either stearoyl-CoA, Δ^6- or Δ^9-octadecenoyl-CoAs in coupled rat heart (solid bars) or rat liver (hatched bars) mitochondria. Values are means ± standard deviations based on at least three measurements. For details see Experimental Procedures. C_{18}, stearoyl-CoA; 9(Z)C_{18}, 9-*cis*-octadecenoyl-CoA; 9(E)C_{18}, 9-*trans*-octadecenoyl-CoA; 6(Z)C_{18}, 6-*cis*-octadecenoyl-CoA; 6(E)C_{18}, 6-*trans*-octadecenoyl-CoA.

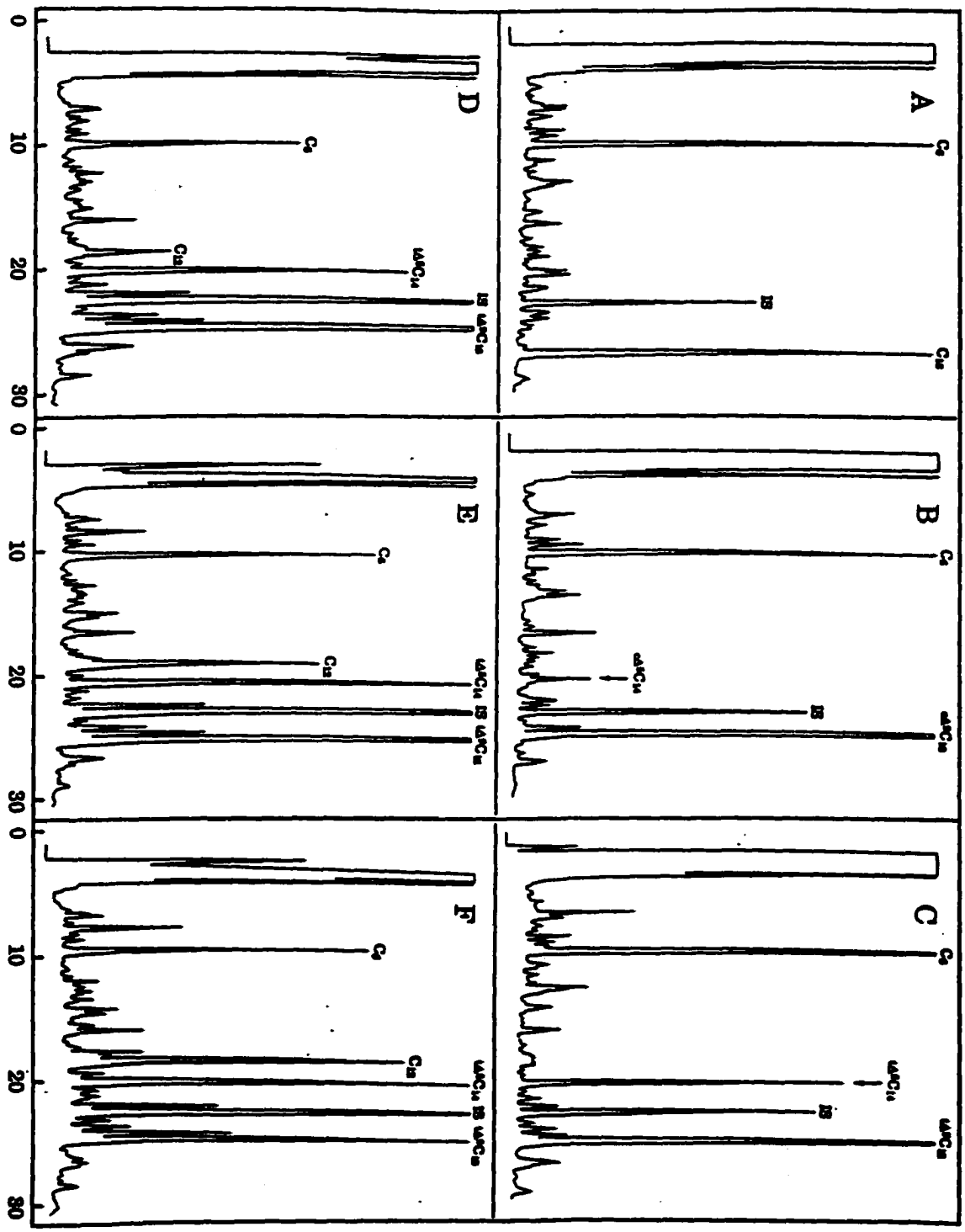

Figure 22. Comparison of metabolic intermediates formed from stearoyl-CoA, oleoyl-CoA and elaidoyl-CoA (panels A, B, and C), and time course of oxidation of elaidoyl-CoA (panels D, E, and F) in coupled rat liver mitochondria. Panel A, 1 min incubation of mitochondria with stearoyl-CoA. Panel B, 1 min incubation with oleoyl-CoA. Panel C, 1 min incubation with elaidoyl-CoA. Panel D, E, and F, oxidation of elaidoyl-CoA for 1.5, 2.5 and 6 min, respectively. C_6, hexanoyl-CoA; C_{12}, dodecanoyl-CoA; IS, internal standard of pentadecanoyl-CoA; C_{18}, stearoyl-CoA; $c\Delta^5C_{14}$, 5-*cis*-tetradecenoyl-CoA; $c\Delta^9C_{18}$, oleoyl-CoA; $t\Delta^5C_{14}$, 5-*trans*-tetradecenoyl-CoA; $t\Delta^9C_{18}$, elaidoyl-CoA.

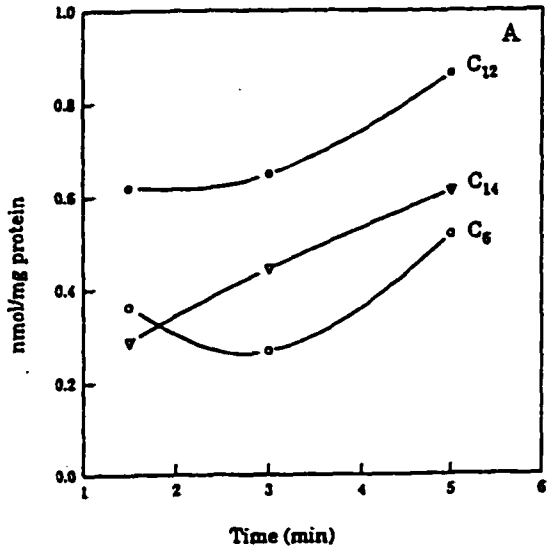

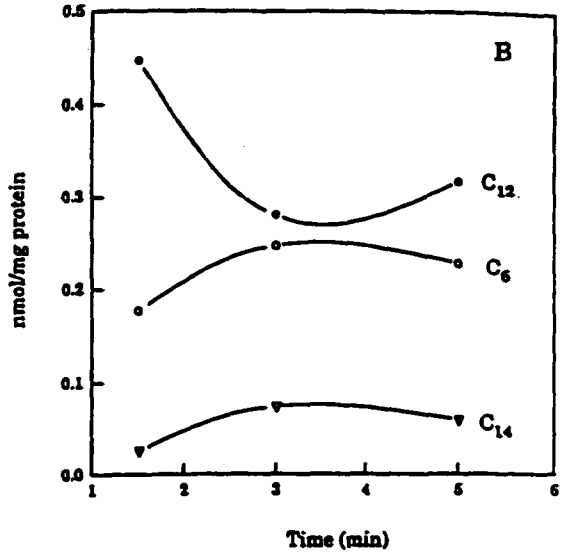

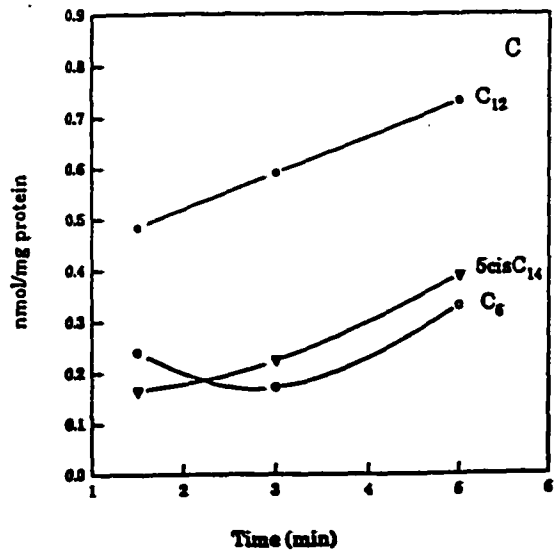

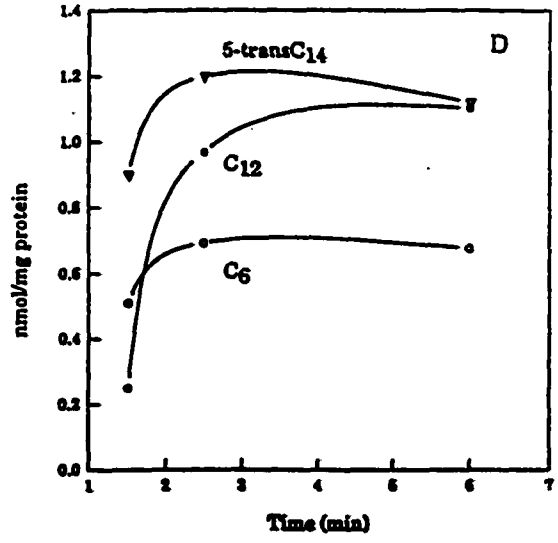

Figure 23. Quantification of metabolites formed during the oxidation of palmitoyl-CoA (panel A), stearoyl-CoA (panel B), oleoyl-CoA (panel C), and elaidoyl-CoA (panel D) as a function of time. C_6, hexanoyl-CoA; C_{12}, dodecanoyl-CoA; 5cisC_{14}, 5-*cis*-tetradecenoyl-CoA; 5-transC_{14}, 5-*trans*-tetradecenoyl-CoA.

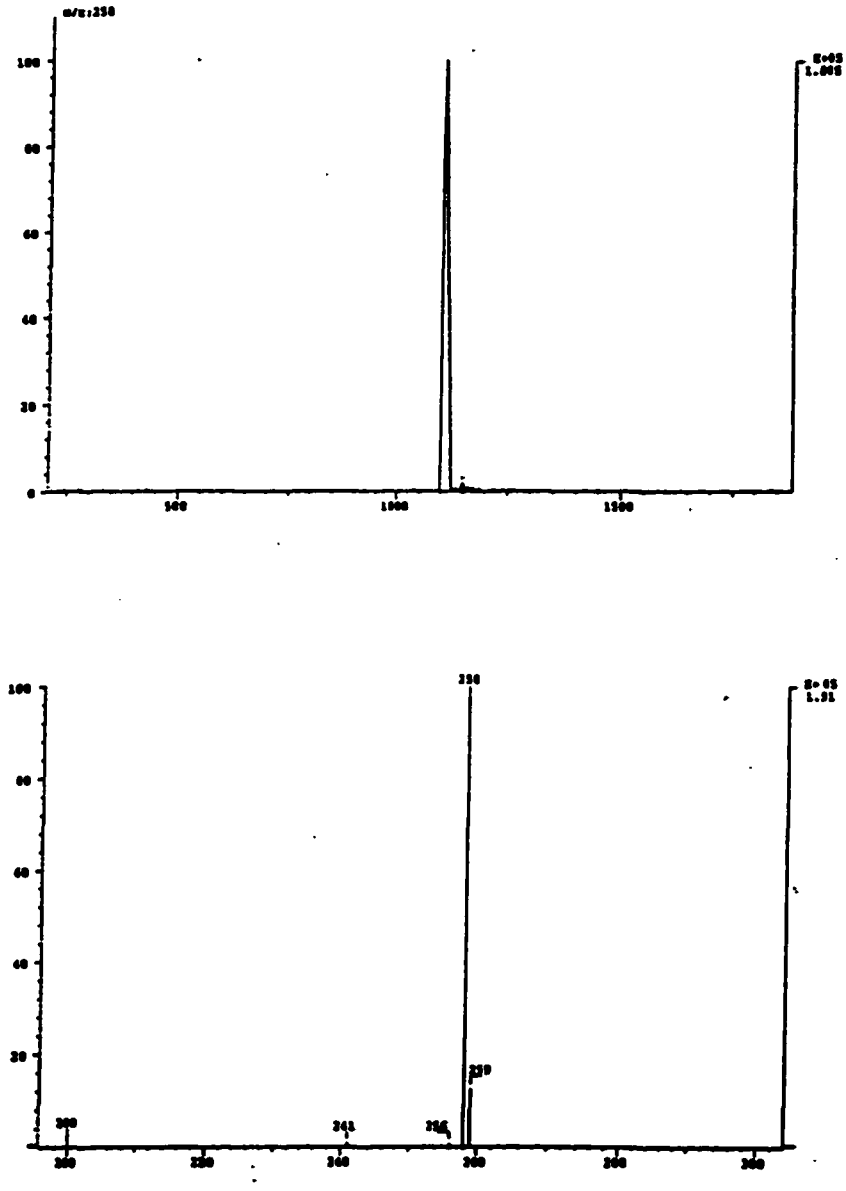

Figure 24. Identification of 5-*trans*-tetradecenoyl-CoA by GC-MS. Panel A, GC spectrum of 5-*trans*-tetradecenoic acid methyl ester. Panel B, MS spectrum of 5-trans-tetradecenoic acid methyl ester with ammonium as a carrier gas.

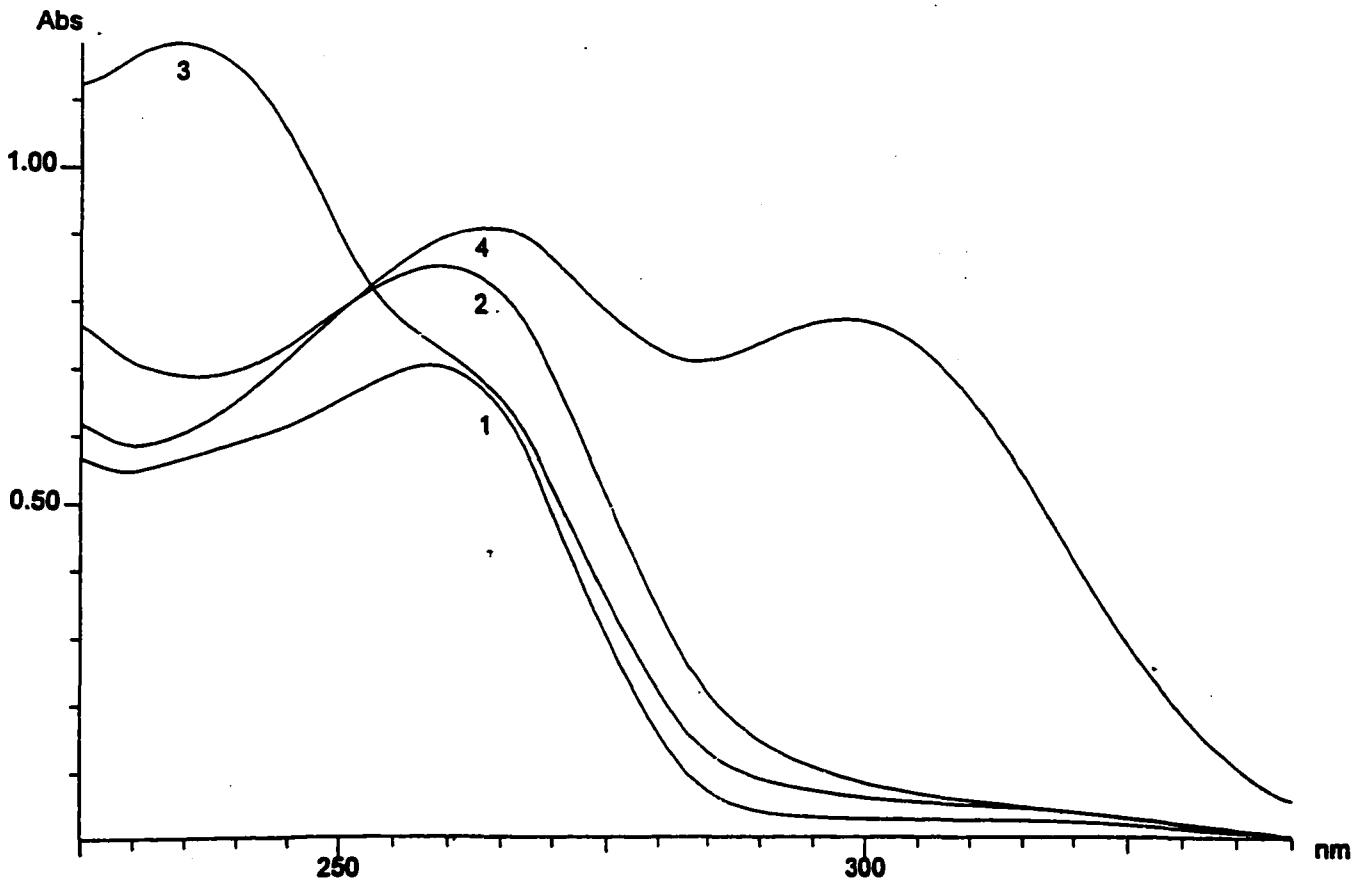

Figure 25. Enzymatic conversions of the compound suspected to be 5-*trans*-tetradecenoyl-CoA. Spectrum 1, 5-*trans*-tetradecenoyl-CoA collected from HPLC. Spectrum 2, after dehydrogenation of 5-*trans*-tetradecenoyl-CoA by 0.1 U of acyl-CoA oxidase; Spectrum 3, after isomerization of 2-*trans*,5-*trans*-tetradecadienoyl-CoA to 3-*trans*,5-*trans*-tetradecadienoyl-CoA by 8 mU of rat liver Δ^3,Δ^2-enoyl-CoA isomerase; Spectrum 4, after isomerization of 3,5-tetradecadienoyl-CoA to 2,4-tetradecadienoyl-CoA by 4 mU of $\Delta^{3,5},\Delta^{2,4}$-dienoyl-CoA isomerase from rat liver.

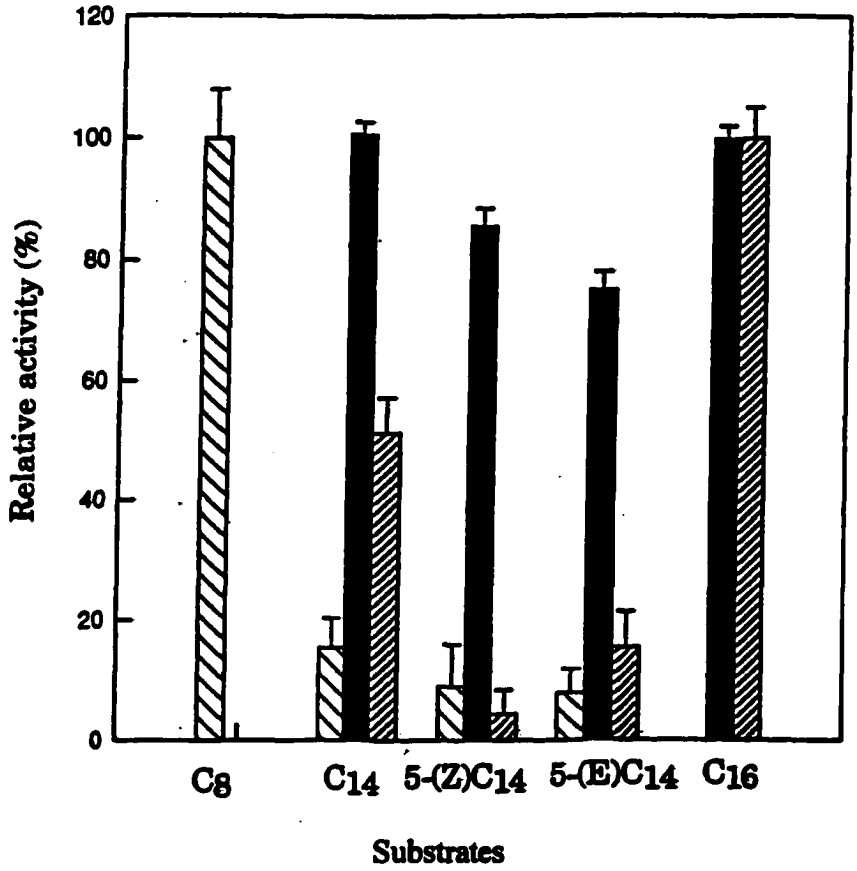

Figure 26. Relative activities of various acyl-CoA dehydrogenases with selected substrates. Medium-chain acyl-CoA dehydrogenase from rat liver (open bars); long-chain acyl-CoA dehydrogenase from rat liver (solid bars); very long-chain acyl-CoA dehydrogenase from rat liver (hatched bars). C_8, octanoyl-CoA; C_{14}, tetradecanoyl-CoA; 5-(Z)C_{14}, 5-*cis*-tetradecenoyl-CoA; 5-(E)-C_{14}, 5-*trans*-tetradecenoyl-CoA.

REFERENCES

1. Kunau, W.-H., Dommes, V., and Schulz, H. (1995) *Prog. Lipid Res.* 34, 267-342.
2. Izai, K., Uchida, Y., Orii, T., Yamamoto, S., and Hashimoto, T. *J. Biol. Chem.* 267, 1027-1033 (1992).
3. Beinert, H. In *The Enzymes* Vol. 7, pp. 447-466 (Boyer, P.D., Lardy, H., and Myrbäck, K. eds) 2nd Edn. Academic Press, New York, 1963.
4. Furuta, S., Miyazawa, S., and Hashimoto, T. (1981) *J. Biochem.* 90, 1739-1750.
5. Yao, K.-W., and Schulz, H. (1996) *J. Biol. Chem.* 271, 17816-17820.
6. Roe, C.R., and Coates, P.M. (1995) in *The Metabolic and Molecular Basis of Inherited Disease* (Scriver, C.R., Beaudet, A.L., Sly, W.S., and Valle, D., Eds.) 7th ed., Vol. I, pp 1501-1533, McGraw-Hill, New York.
7. Stoffel, W. and Grol, M. (1978) *Hoppe-Seyler's Z. Physiol. Chem.* 359, 1777-1782.
8. Palosaari, P. M., Kilponen, J. M., Sormunen, R. T., Hassinen, I. E. and Hiltunen, J. K. (1990) *J. Biol. Chem.* 265, 3347-3353.
9. Euler-Bertram, S. and Stoffel, W. (1990) *Biol. Chem. Hoppe-Seyler* 371, 603-610.
10. Dommes, V., Luster, W., Cvetanovic, M., and Kunau, W-H. (1982) *Eur. J. Biochem.* 125, 335-341.
11. Luo, M.J., Smeland, T.E., Shoukry, K., and Schulz, H. (1994) *J. Biol. Chem.* 269, 2384-2388.
12. Wang, H.-Y. and Schulz, H. (1989) *Biochem. J.* 264, 47-52.
13. Dommes, V., and Kunau, H. (1984) *J. Biol. Chem.* 259, 1781-1788.
14. He, X.-Y., Yang, S.-Y., and Schulz, H. (1997) *Eur. J. Biochem.* 248, 516-520.

15. Mizugaki, M., Kimura, C., Kondo, A., Kawaguchi, A., Okuda, S., and Yamanaka, H. (1984) *J. Biochem.* 95, 311-317.

16. Mizugaki, M., Kimura, C., Nishimaki, T., Kawaguchi, A., Okuda, S., and Yamanaka, H. (1983) *J. Biochem.* 94, 409-413.

17. Dutton, H.J. (1979) in *Geometrical and Positional Fatty Acid Isomers* (Emken, E.A. and Dutton, H.J., eds.) pp. 1-16, The American Oil Chemists' Society, Champaign, Illinois.

18. Kepler, C.R., Hirons, K.P., McNeil, J.J., and Tooe, S.B. (1966) *J. Biol. Chem.* 241, 1350-1354.

19. Osumi, T., and Hashimoto, T. (1979) *Biochem. Biophys. Res. Commun.* 89, 580-584.

20. Palosaari, P.M. and Hiltunen, J.K. (1990) *J. Biol. Chem.* 265, 2446-2449.

21. Steinman, H. and Hill, R.L. (1965) *Methods Enzymol.* 35, 136-151.

22. Bradshaw, R.A. and Noyes, B.E. (1975) *Methods Enzymol.* 35, 136-151.

23. Smeland, T.E., Nada, M., Cuebas, D., and Schulz, H. (1992) *Proc. Natl. Acad. Sci. U.S.A.* 89, 6673-6677.

24. Thomason, S.C., and Kubler, D.G. (1968) *J. Chem. Educ.* 45, 546-547.

25. Linstead, R.P., Noble, E.G., and Boorman, E.G. (1933) *J. Chem. Soc.*, 557-561.

26. Fong, J.C., and Schulz, H. (1981) *Methods Enzymol.* 71, 390-398.

27. Ellman, G.L. (1959) *Arch. Biochem. Biophys.* 82, 70-77.

28. Thorpe, C. (1986) *Anal. Biochem.* 155, 391-394.

29. Yang, S.-Y., Cuebas, D., and Schulz, H. (1986) *J. Biol. Chem.* 261, 12238-12243.

30. Nada, M.A., Shoukry, K., and Schulz, H. (1994) *Lipids*, 29, 517-521.

31. Shoukry, K. and Schulz, H. (1998) *J. Biol. Chem.* 273, 6892-6899.

32. Stotter, P.L., and Hill, K.A. (1975) *Tetrahedron Lett.*, 1679-1682.

33. Isler, O., Gutmann, H., Montavon, M., Rüegg, R., Ryser, G., and Zeller, P. (1957) *Helv. Chim. Acta 40*, 1242-1249.

34. Dauben, W.G., Gerdes, J.M., and Bunce, R.A. (1984) *J. Org. Chem.* 49, 4293-4295.

35. Löffler, A., Pratt, R.J., Rüesch, H.P., and Dreiding, A.S. (1970) *Helv. Chim. Acta* 53, 383-403.

36. Maryanoff, B.E., Reitz, A.B., and Duhl-Emswiler, B.A. (1985) *J. Am. Chem. Soc.* 107, 217-226.

37. Nedergaard, J., and Cannon, B. (1979) *Methods Enzymol.* 71, 390-398.

38. Chappell, J.B. and Hansford, R.G. (1969) in *Subcellular Components* (Birnie, G. D., ed.), 2nd eds., pp.77-91, Butterworth, London.

39. Bradford, M.M. (1976) *Anal. Biochem.* 72, 248-254.

40. Olowe, Y., and Schulz, H. (1982) *J. Biol. Chem.* 257, 5408-5413.

41. Binstock, J.F., and Schulz, H. (1981) *Methods Enzymol.* 71, 403-411.

42. Kunau, W.H., and Dommes, P. (1978) *Eur. J. Biochem.* 91, 533-544.

43. Koziol, J. (1971) *Methods Enzymol.* 18, 273.

44. Faeder, E.J., and Siegel, L.M. (1973) *Anal. Biochem.* 53, 332-336.

45. Vanoni, M.A., Edmondson, D.E., Zanetti, G., and Curti, B. (1992) *Biochemistry*, 31, 4613-4623.

46. Brumby, P.E., Miller, R.W., and Massay, V. (1965) *J. Biol. Chem.* 240, 2222-2228.

47. Williams, C.H., Arscott, L.D., Matthews, R.G., Thorpe, C., & Wilkinson, K.D. (1979) *Methods Enzymol.* 62D, 185-198.

48. Massay, V., and Hemmerich, P. (1978) *Biochemistry* 17, 9-17.

49. Thorpe, C., Mattews, R.G., and Williams, C.H. (1979) *Biochemistry* 18, 331-337.

50. Mizzer, J.P., and Thorpe, C. (1981) *Biochemistry*, 20, 4965-4970.

51. Mao, L.-F., Chu, M.J., Simon, A., Abbas, A.S., and Schulz, H. (1995) *Arch. Biochem. Biophys.* 321, 221-228.

52. D'Ordine, R.L., Tonge, P.J., Carey, P.R., and Anderson, V.E. (1994) *Biochemistry*, 33, 12635-12643.

53. Dahl, K.H., and Dunn, M.F. (1984) *Biochemistry*, 23, 4094-4100.

54. Dunn, E.F., and Bukley, P.D. (1985) in *Enzymololgy of Carbonyl Metabolism 2: Aldehyde Dehydrogenase, and Aldo/Keto Reductase and Alcohol Dehydrogenase*, pp 15-27, Alan R. Liss Publishers, New York.

55. Schulz, H. (1991) *Biochim, Biophys. Acta* 1081, 109-120.

56. Schulz, H. (1990) in *Fatty Acid Oxidation: Clinical, Biochemical, and Molecular Aspects* (Tanaka, K., and Coates, P. M., Eds.) pp 153-165, Alan R. Liss, Inc., New York.

57. Li, J., and Schulz, H. (1988) *Biochemistry* 27, 5995-6000.

58. Miyazawa, S., Furuta, S., Osumi, T., Hashimoto, T., and Ui, N. (1981) *J. Biochem.* 90, 511-519.

59. He, X.-Y., Shoukry, K., Chu, C., Yang, J., Sprecher, H., and Schulz, H. (1995) *Biochem. Biophys. Res. Commun.* 215, 15-22.

60. Filppula, S.A., Yagi, A.I., Kilpeläinen, S.H., Novikov, D., FitzPatrick, D.R., Vihinen, M., Valle, D., and Hiltunen, J.K. (1998) *J. Biol. Chem.* 273, 349-355.

61. Chen, L.-S., Jin, S.-J., and Tserng, K.-Y. (1994) *Biochemistry*, 33, 10527-10534.

62. Modis, Y., Filppula, S.A, Novikov, D.K, Norledge, B., Hiltunen, J.K., and Wierenga, R.K. (1998) *Structure*, 6, 957-970.

63. Carey, P.R., and Tonge, P.J. (1995) *Acc. Chem. Res.*, 28, 8-13.

64. Austin, J.C., Kuliopoulos, A., Mildvan, A.S., and Spiro, T.G. (1992) *Protein Sci.* 1, 259-270.

65. Kuno, S., Bacher, A., and Simon, H. (1985) *Biol. Chem. Hoppe-Seyler* 366, 463472.

66. Caldeira, J., Feicht, R., White, H., Teixeira, M., Moura, J.J.G., Simon, H., and Moura, I. (1996) *J. Biol. Chem.* 271, 18743-18748.

67. Willebrands, A.F. and Van Der Veen, K.J. (1966) *Biochim. Biophys. Acta.* 116, 583-585.

68. Stanley, K.K. and Tubbs, P.K. (1975) *Biochem. J.* 150, 77-88.